

1 Leaf ontogeny steers ethylene and auxin crosstalk to  
2 regulate leaf epinasty during waterlogging of  
3 tomato

4

5 Geldhof B.<sup>1</sup>, Pattyn J.<sup>1</sup>, Mohorović P.<sup>1</sup>, Van den Broeck K.<sup>1</sup>, Everaerts V.<sup>1</sup>, Novák O.<sup>2</sup>, Van de Poel B.<sup>1,3,\*</sup>

6 <sup>1</sup> Molecular Plant Hormone Physiology Lab, Division of Crop Biotechnics, Department of Biosystems, KU Leuven, Willem de  
7 Croylaan 42, Leuven 3001, Belgium

8 <sup>2</sup>Laboratory of Growth Regulators, Centre of the Region Haná for Biotechnological and Agricultural Research, Institute of  
9 Experimental Botany, Czech Academy of Sciences, and Faculty of Science, Palacký University, CZ-783 71 Olomouc, Czech Republic

10 <sup>3</sup> KU Leuven Plant Institute (LPI), KU Leuven, Arenbergpark 30, 3001 Leuven, Belgium

11

12 \*Author for correspondence: Bram Van de Poel – [bram.vandepoel@kuleuven.be](mailto:bram.vandepoel@kuleuven.be)

13

14 ORCIDs:

- 15 - Batist Geldhof: 0000-0003-0025-1750
- 16 - Jolien Pattyn: 0000-0001-5269-2799
- 17 - Petar Mohorović: 0000-0002-3368-3974
- 18 - Ondřej Novák: 0000-0003-3452-0154
- 19 - Bram Van de Poel: 0000-0001-5638-2472

20

21

## 22 Abstract

23 Developing leaves undergo a vast array of age-related changes as they mature. These include  
24 physiological, hormonal and morphological changes that determine their adaptation plasticity towards  
25 adverse conditions. Waterlogging induces leaf epinasty in tomato, and the magnitude of leaf bending is  
26 intricately related to the age-dependent cellular and hormonal response. We now show that ethylene,  
27 the master regulator of epinasty, is differentially regulated throughout leaf development, giving rise to  
28 age-dependent epinastic responses. Young leaves have a higher basal ethylene production, but are less  
29 responsive to waterlogging-induced epinasty, as they have a higher capacity to convert the root-borne  
30 and mobilized ACC into the inactive conjugate MACC. Ethylene stimulates cell elongation relatively more  
31 at the adaxial petiole side, by activating auxin biosynthesis and locally inhibiting its transport through PIN4  
32 and PIN9 in older and mature leaves. As a result, auxins accumulate in the petiole base of these leaves  
33 and enforce partially irreversible epinastic bending upon waterlogging. Young leaves maintain their  
34 potential to transport auxins, both locally and through the vascular tissue, leading to enhanced flexibility  
35 to dampen the epinastic response and a faster upwards repositioning during reoxygenation. This  
36 mechanism also explains the observed reduction of epinasty during and its recovery after waterlogging in  
37 the *anthocyanin reduced (are)* and *Never ripe (Nr)* mutants, both characterized by higher auxin flow. Our  
38 work has demonstrated that waterlogging activates intricate hormonal crosstalk between ethylene and  
39 auxin, controlled in an age-dependent way.

## 40 Keywords

41 Epinasty, waterlogging, ontogeny, ethylene, auxin, tomato

42

## 43 Introduction

44 Plants have developed several strategies to cope with low oxygen stress induced by flooding and  
45 submergence (Sasidharan et al., 2017). Morphological changes include escape responses such as  
46 hyponasty (Cox et al., 2003) and shoot elongation (Kende et al., 1998; Voesenek et al., 2004) to restore  
47 connectivity with the air. Other adaptations enhance the uptake and transport of oxygen through the  
48 formation of aerenchyma (Evans, 2004), adventitious roots (Vidoz et al., 2016) or hypertrophic lenticels  
49 (Shimamura et al., 2010). One of the more enigmatic responses caused by root anaerobiosis is the  
50 downward bending of leaves, called leaf epinasty. This nastic movement has been observed in several  
51 crops such as tomato (Jackson & Campbell, 1976), potato (Tonneijck et al., 1999), sunflower (Kawase,  
52 1974) and cotton (Wiese & Devay, 1970). It is hypothesized that epinasty is an avoidance strategy to  
53 minimize intense solar radiation (Van Geest et al., 2012) and reduce plant transpiration (Else et al., 2009;  
54 Grichko & Glick, 2001).

55 A long time ago, exogenous ethylene was described to cause leaf epinasty in tomato (*Solanum*  
56 *lycopersicum*) (Doubt, 1917). Later, Jackson and Campbell (1976) established the relationship between  
57 waterlogging and an increase in ethylene production causing epinasty. Soon thereafter, it was shown that  
58 hypoxic conditions in the rooting zone induce both the production and transport of 1-aminocyclopropane-  
59 1-carboxylic acid (ACC), the immediate precursor of ethylene (Bradford & Yang, 1980). In tomato, ACC  
60 accumulates in hypoxic roots due to the upregulation of *ACC SYNTHASE7 (ACS7)* (Shiu et al., 1998), *ACS2*  
61 and *ACS3* (Olson et al., 1995). Subsequently, ACC is transported by the xylem (Bradford & Yang, 1980a) to  
62 the normoxic shoot, where it is converted into ethylene (English et al., 1995) by *ACC OXIDASE1 (ACO1)*,  
63 causing the epinastic response (English et al., 1995).

64 Besides ethylene, other signaling molecules such as auxins (Keller & Van Volkenburgh, 1997; Sandalio et  
65 al., 2016), calcium (Lee et al., 2008) and radical oxygen species (ROS) (Pazmiño et al., 2014; Pazmiño et  
66 al., 2011) have been linked to epinastic movements of the leaf petiole and rachis. During leaf epinasty,  
67 both auxins (Lyon, 1963a, 1963b) and calcium are redistributed across the petiole (Lee et al., 2008),  
68 causing the cells on the adaxial side to elongate (Kazemi & Kefford, 1974; Ursin & Bradford, 1989a).

69 Early work has shown that auxins, besides ethylene, can evoke a strong epinastic response in tomato (Lyon,  
70 1963). So far, it remains unknown if auxins act only through the induction of ethylene or not (Keller & Van  
71 Volkenburgh, 1997; Sandalio et al., 2016; Ursin & Bradford, 1989a). While auxins can induce epinasty in  
72 the presence of ethylene biosynthesis inhibitors (Keller & Van Volkenburgh, 1997) or in ethylene

73 insensitive mutants (Romano et al., 1993), insensitivity to auxins in the auxin-resistant *diageotropica (dgt)*  
74 mutant does not impede epinasty after an ethylene treatment (Ursin & Bradford, 1989a). Although the  
75 interplay between both hormones is complex, ethylene has been described as a mediator of auxin  
76 biosynthesis, transport and signaling in other plant processes (Muday et al., 2012). SIIAA3, an Aux/IAA  
77 transcription factor, was identified as a possible point of crosstalk between auxin and ethylene signaling  
78 during leaf epinasty (Chaabouni et al., 2009). Moreover, both hormones have been associated with the  
79 production of ROS as a regulator of epinastic bending (Pazmiño et al., 2014).

80 Despite the identification of several signaling molecules involved in epinastic movements, their crosstalk  
81 and their action during flooding remain elusive. Furthermore, it is not known how leaves of different  
82 developmental stages respond to waterlogging and if there is an ontogenic hormonal regulation of leaf  
83 epinasty. In this study, we untangle the crosstalk between ethylene and auxin and assess how leaves of  
84 different ages respond to waterlogging and reoxygenation, especially in terms of epinasty.

## 85 **Materials and methods**

### 86 **Plant material and growth conditions**

87 Tomato (*Solanum lycopersicum*) seeds of the cultivar Ailsa Craig and the *Never ripe (Nr)* mutant were  
88 germinated in soil and later transferred to rockwool blocks. Seeds of the *SIPIN4-RNAi* and *pDR5::GUS*  
89 tomato lines were kindly provided by Prof. Carmen Catalá (Pattison & Catalá, 2012). The *are* mutant was  
90 kindly provided by Prof. Gloria Muday (Maloney et al., 2014). Tomato plants were grown in individual  
91 trays in a growth chamber or a greenhouse. The growth chamber had a temperature of 21 °C during the  
92 day and 18 °C during the night with a constant relative humidity of 65 %. Light was given in a 16 h/8 h  
93 day/night cycle using VS12 solar-spectrum mimicking LED lamps (Sunritec, China) with an intensity of 120  
94  $\mu\text{mol s}^{-1} \text{m}^{-2}$ . In the greenhouse, the temperature was set at 18 °C during day and night with a humidity  
95 between 65 % and 70 %. In case the solar light intensity dropped below 250  $\text{W m}^{-2}$  additional illumination  
96 was provided with high-pressure sodium lamps (SON-T). All plants received fertigation solution in their  
97 trays (growth chamber) or through drip irrigation (greenhouse).

### 98 **Waterlogging treatment**

99 Tomato plants were grown until the eighth leaf stage. Subsequently, plants were transferred to individual  
100 trays filled with distilled water up to four cm above the rockwool surface to induce root hypoxia through  
101 natural oxygen consumption. During this period of waterlogging, the oxygen concentration in the root  
102 zone was monitored with an optical oxygen sensor (FireStingO<sub>2</sub> Pyroscience). The hypoxia treatment

103 started at 9 AM (1 – 2 h zeitgeber time) and was maintained for 24 to 96 h, after which the plants were  
104 removed from the trays to allow reoxygenation.

### 105 Petiole morphology and epidermal anatomy

106 Leaf angles between the adaxial side of the petiole and the stem were measured with a protractor or a  
107 leaf angle sensor at the first two cm of the petiole base (described in Geldhof et al. (2021)). The length of  
108 petiole segments was measured between one and two centimeter marks at the petiole base.  
109 Subsequently, epidermal imprints were taken of the adaxial and abaxial side of the petioles after  
110 application of nail polish (Maybelline New York) for one hour. These imprints were visualized using an  
111 Olympus BX40 microscope and cell lengths were quantified in ImageJ.

### 112 Plant and leaf physiology

113 Whole plant transpiration was measured using 24 digital lysimeters (KB 2400-2N scales, Kern) with a  
114 logging frequency of 10 s. Canopy cover changes were quantified through analysis of top view images  
115 (Nikon D3200) in ImageJ. Total plant CO<sub>2</sub> consumption rate was monitored with SCD30 CO<sub>2</sub> sensors  
116 (Sensirion) for individual plants in airtight PMMA boxes, flushed via an automated stop-and-flow system  
117 with a CO<sub>2</sub> concentration between 400 and 600 ppm during the day. The maximum quantum yield of PSII  
118 ( $F_v/F_m$ ) was measured on individual leaves with a continuous excitation chlorophyll fluorimeter (Handy  
119 Pea, Hansatech) after 30 min dark adaptation. Leaf photosynthesis, stomatal conductance and  
120 transpiration were determined for leaflet patches with an LCi compact portable photosynthesis system  
121 (ADC Bioscientific). Leaf fresh and dry weight were determined at different time points during  
122 waterlogging and subsequent reoxygenation.

### 123 Ethylene measurements

124 Ethylene production of individual leaf petioles was determined by gas chromatography (GC-2010  
125 Shimadzu). Two petiole sections of approximately 3 cm were sampled and incubated together in 5 mL  
126 cuvettes for 30 min (five replicates per treatment). Afterwards, the cuvettes were flushed to remove  
127 (wound) ethylene and sampled hourly following the same procedure. Ethylene measurements were  
128 performed for leaf 3, 5 and 7. Data was normalized for petiole fresh and dry weight.

### 129 Histochemical staining of EBS::GUS and DR5::GUS

130 GUS activity was assessed following the protocol by Blakeslee and Murphy (2016). Petiole/stem segments  
131 of three cm were washed in buffer solution and vacuum infiltrated for 10 – 60 min in staining solution (1  
132 mM X-Gluc; 100 mM sodium phosphate, pH 7; 10 mM EDTA; 0.5 mM potassium ferricyanide; 0.5 mM

133 potassium ferrocyanide; 0.1 % Triton X-100), followed by 4 – 5 h (EBS::GUS) or overnight (DR5::GUS)  
134 incubation at 37 °C and clearing in 90 % ethanol:water (v/v). Petiole sections were visualized using an  
135 Olympus BX40 microscope and DR5::GUS staining was quantified by image analysis using a Python  
136 pipeline. Generation of the EBS::GUS reporter line is described in Supporting Information Method S1.

### 137 1-MCP and TIBA treatments

138 For the 1-methylcyclopropene (1-MCP) treatment, plants were transferred to airtight PMMA boxes the  
139 evening before the start of waterlogging. Each box contained three plants and half of the boxes were pre-  
140 treated with 1 ppm 1-MCP. For the 2,3,5-triiodobenzoic acid (TIBA) treatment, plants were sprayed with  
141 1 mM TIBA and 0.05 % TWEEN-20 in water until runoff the evening before waterlogging. Control plants  
142 were sprayed with a 0.05 % TWEEN-20 water solution. Alternatively, TIBA was suspended in ethanol and  
143 lanolin (1 % m/m) and applied as a 0.5 – 1 cm ring around the leaf petiole.

### 144 RNA extraction and RT-qPCR

145 Tomato leaves were snap frozen and ground in liquid nitrogen. RNA was extracted using the GeneJET Plant  
146 RNA Purification Mini Kit protocol (Thermo Scientific). DNA was removed using the RapidOut DNA  
147 Removal Kit (Thermo Scientific). Total RNA yield was assessed on the Nanodrop (Nanodrop Technology)  
148 and RNA quality was verified through gel electrophoresis. cDNA was synthesized using the iScript cDNA  
149 Synthesis Kit protocol (BIO-RAD). RT-qPCR was performed with a CFX96 (BIO-RAD) for 35 cycles. Four  
150 reference genes were selected based on earlier findings (Van de Poel et al., 2012) for normalization.  
151 Primers are listed in Supporting Information Table S1.

### 152 ACC and MACC quantification

153 ACC and malonyl-ACC (MACC) content of different leaves were assessed based on the protocol described  
154 by Bulens et al. (2011) based on the Lizada & Yang (1979) method.

### 155 ACO activity and abundance

156 ACO activity was derived from the *in vitro* ethylene production in airtight headspace vials, following Bulens  
157 et al. (2011). ACO was extracted using a modified protocol of Ververidis *et al.* (1991) as described by  
158 Mathooko *et al.* (1995) and Castellano *et al.* (2002). The ethylene content in the headspace was measured  
159 with a gas chromatograph (GC-2014 Shimadzu). Total ACO abundance was quantified using western-  
160 blotting according to Van de Poel et al. (2014), using a custom-made anti-ACO antibody targeting a  
161 conserved (ACO1-4) epitope.

## 162 AMT activity

163 ACC-N-malonyl transferase (AMT) activity was derived from the *in vitro* MACC formation. AMT was  
164 extracted from snap-frozen crushed tissue (0.5 g) in 500  $\mu$ L extraction buffer (200 mM Tris-Cl pH 8; 4 mM  
165 EDTA pH 8.5; 10 mM DTT; 2 mM benzamidine; 2 mM 6-amino-n-hexanoic acid; 0.5 mM N- $\alpha$ -p-tosyl-L-  
166 arginine methyl ester hydrochloride; 6  $\mu$ M pepstatin; 2  $\mu$ M leupeptin; 2 mM phenylmethanesulfonyl  
167 fluoride). After 30 minutes of incubation on ice and intermittent vortexing, the samples were centrifuged  
168 at 17.000 x g at 4  $^{\circ}$ C for 10 minutes. Next, 20  $\mu$ L of the supernatant was added to 30  $\mu$ L reaction mix (2  
169 mM ACC; 0.5 mM malonyl-coA; 100 mM Tris-Cl pH 8; 1 mM DTT and 1 mM EDTA) and incubated for 3 h  
170 at 30  $^{\circ}$ C, followed by enzyme deactivation at 100  $^{\circ}$ C for 5 min. After removal of residual ACC by a cation  
171 exchanger (Dowex cation exchange column; 50WX8, 100-200 mesh), MACC was converted into ACC and  
172 subsequently converted into ethylene according to the protocol of Bulens et al. (2011).

## 173 Auxin quantification

174 The auxin precursors tryptophan (TRP), tryptamine (TRA) and anthranilate (ANT), and IAA and its  
175 catabolite oxIAA were quantified in leaves and 2 cm petiole segments after 12 h, 24 h and 48 h of  
176 waterlogging (5 replicates per treatment). Leaves and petioles (leaf 1, 3, 5 and 7) were snap frozen,  
177 pulverized and analyzed following an UHPLC-ESI-MS/MS protocol described in Šimura et al. (2018).

## 178 Statistical analysis

179 All analyses and visualizations were carried out in R. Treatments were compared using a Wilcoxon test for  
180 paired samples ( $\alpha = 0.05$ ) or a Dunn's test with Bonferroni connection for multiple comparisons ( $\alpha = 0.05$ ).  
181 Empirical cumulative distributions (ECD) of cell lengths were compared using a Kolmogorov-Smirnov test  
182 ( $\alpha = 0.05$ ).

## 183 Results

### 184 Waterlogging-induced epinasty is leaf age-dependent

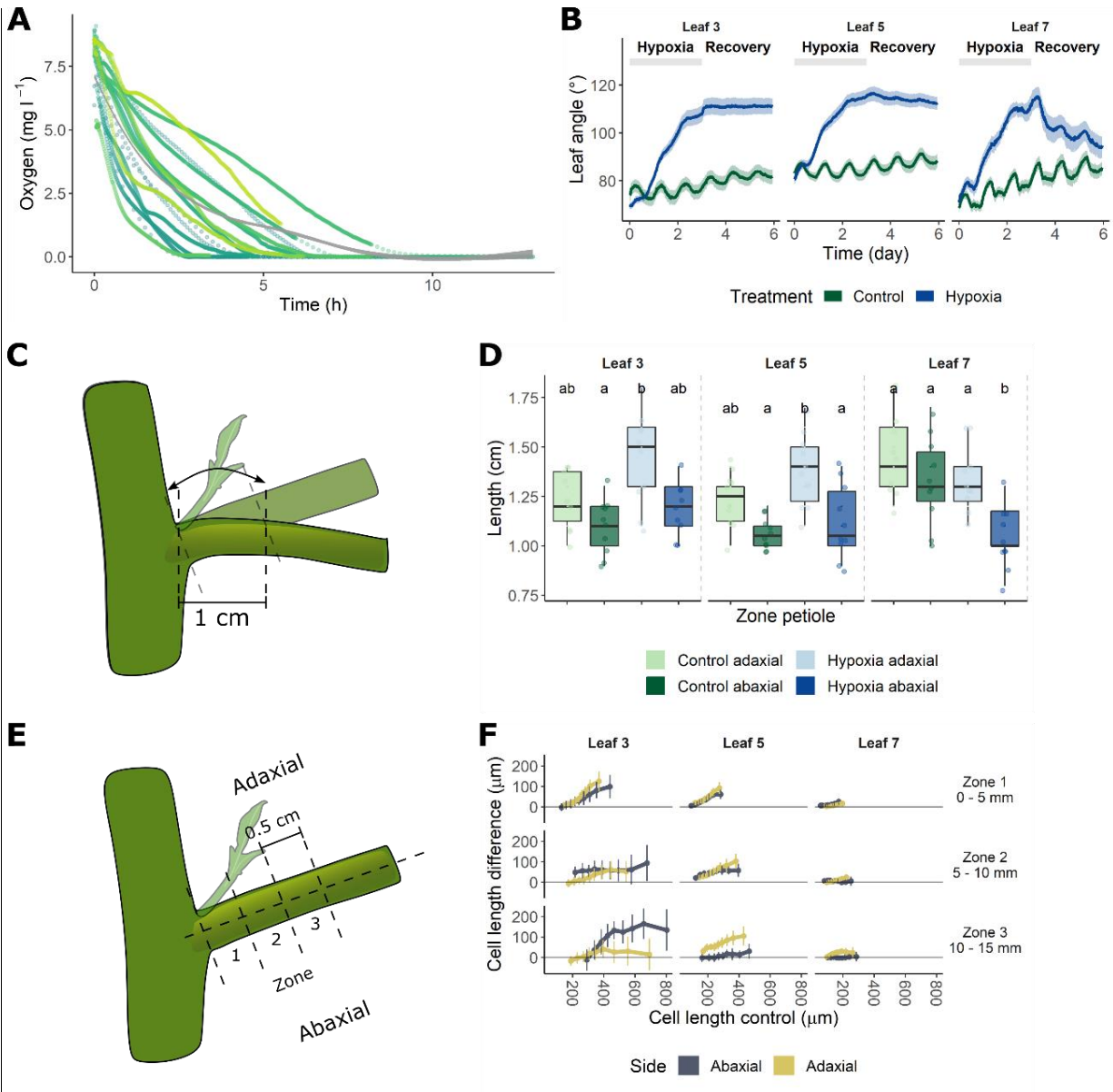
185 Tomato plants exposed to waterlogging show a quick epinastic bending of the leaves. By monitoring leaf  
186 angle dynamics in young tomato plants with 8 leaves, using a real-time clip-on IMU sensor (Geldhof et al.,  
187 2021), we observed an age-dependent (ontogenic) epinastic response towards waterlogging. The rapid  
188 decline of dissolved oxygen in the rooting zone (Figure 1A) caused more prominent downwards bending  
189 in older (leaf 3) and middle-aged (leaf 5) leaves, not recovering after 48 h of reoxygenation (Figure 1B &

190 Supporting Information Fig. S1). Younger leaves (leaf 7) showed a similar epinastic response but were able  
191 to recover during reoxygenation.

192 To further characterize these epinastic movements at the cellular level, we compared the adaxial and  
193 abaxial petiole morphology and anatomy. Adaxial petiole segments of leaf 3 to 6 showed an enhanced  
194 elongation after 48 h of waterlogging, while this was seemingly reduced on the abaxial petiole side of  
195 young leaves (Figure 1C – D & Supporting Information Fig. S1). These variations in petiole elongation could  
196 explain the differences in angular dynamics between leaves. Subsequently, we examined cell dimensions  
197 using epidermal cell imprints. Both the adaxial and abaxial epidermal cell length increased after two days  
198 of root hypoxia, as shown by a significant shift in the empirical cumulative cell length distributions (ECD)  
199 (Figure 1E – G and Supporting Information Fig. S1). The ECD represents the proportion of cells smaller  
200 than or equal to a certain size (Supporting Information Method S3). We did not observe a difference in  
201 ECD for the adaxial side of leaf 8 and the abaxial sides of leaf 2, 7 and 8. In general, this shift suggests that  
202 elongation of cells is more pronounced at the abaxial side of the petiole, except for petiole segments  
203 located close to the stem (Figure 1E – F and Supporting Information Fig. S1).

204 To validate this enhanced abaxial elongation, we subsequently quantified the relative cell elongation  
205 during waterlogging by comparing cell length distribution quantiles in 0.5 cm zones on the adaxial and  
206 abaxial side of the petiole (Figure 1E). For a detailed description of this quantile shift method, we refer  
207 the reader to Supporting Information Method S3. In control conditions, cells at the abaxial side elongated  
208 relatively more than those at the adaxial side. During waterlogging, especially adaxial epidermal cells  
209 became proportionally larger, depending on the position along the petiole as well as leaf age. In addition,  
210 leaf development seemed to limit the extent of the differentiation between adaxial and abaxial epidermis  
211 cells. Altogether, epidermal cell elongation was respectively larger on the adaxial and smaller on the  
212 abaxial side of the petiole during waterlogging, causing downward bending of the petiole.



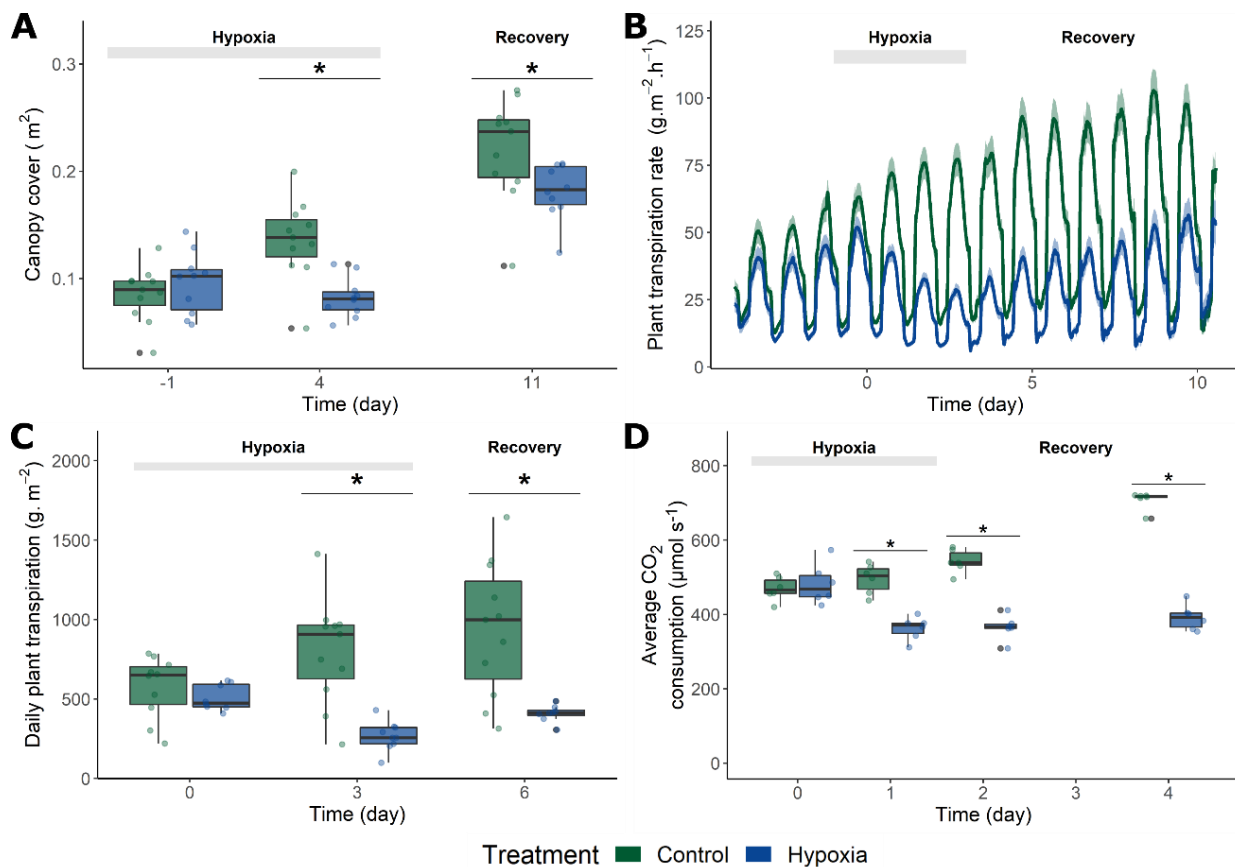


213

214 Figure 1: Ontogenic petiole angle dynamics, morphology and anatomy of tomato (Ailsa Craig; leaf 3, 5 and 7) after a waterlogging  
 215 treatment. (A) Oxygen concentration in the rooting zone during the treatment, together with a smoothed model of the mean.  
 216 Individual lines represent individual  $O_2$  consumption profiles. (B) Epinastic response of leaves of different ages during a 72 h  
 217 waterlogging treatment and subsequent reoxygenation. (C – D) Length of the abaxial and adaxial sides ( $n = 10$ ) of the first cm of  
 218 the petiole after 48 h of treatment. (E – F) Differences in epidermal cell length distributions ( $n = 2 - 631$  cells per treatment and  
 219 zone for the adaxial and abaxial side per plant; 6 – 7 plants per treatment) between 48 h waterlogging and control conditions.  
 220 The different zones in (E – F) refer to regions of the petiole of approximately 5 mm, starting at the petiole base (zone 1) and  
 221 stretching out 15 mm along the petiole (zone 3). Significant differences are indicated with letters ( $\alpha = 0.05$ ).

## 222 Waterlogging reduces whole-plant transpiration and photosynthesis

223 To determine the effect of leaf epinasty on plant performance during waterlogging, we studied several  
 224 physiological responses. Leaf epinasty significantly reduced canopy cover during waterlogging, only partly  
 225 recovering after 7 days of reoxygenation (Figure 2A). Using real-time lysimetry, we observed that whole-  
 226 plant transpiration rate dropped shortly after the start of the hypoxia treatment (31 – 47 % 1 day after  
 227 treatment), and that it did not fully recover during reoxygenation (Figure 2B – C & Supporting Information  
 228 Fig. S2). Accordingly, total plant CO<sub>2</sub> uptake decreased during waterlogging and did not recover during  
 229 reoxygenation (Figure 2D), indicating that both transpiration and photosynthesis are impaired at the onset  
 230 of root hypoxia stress.



231

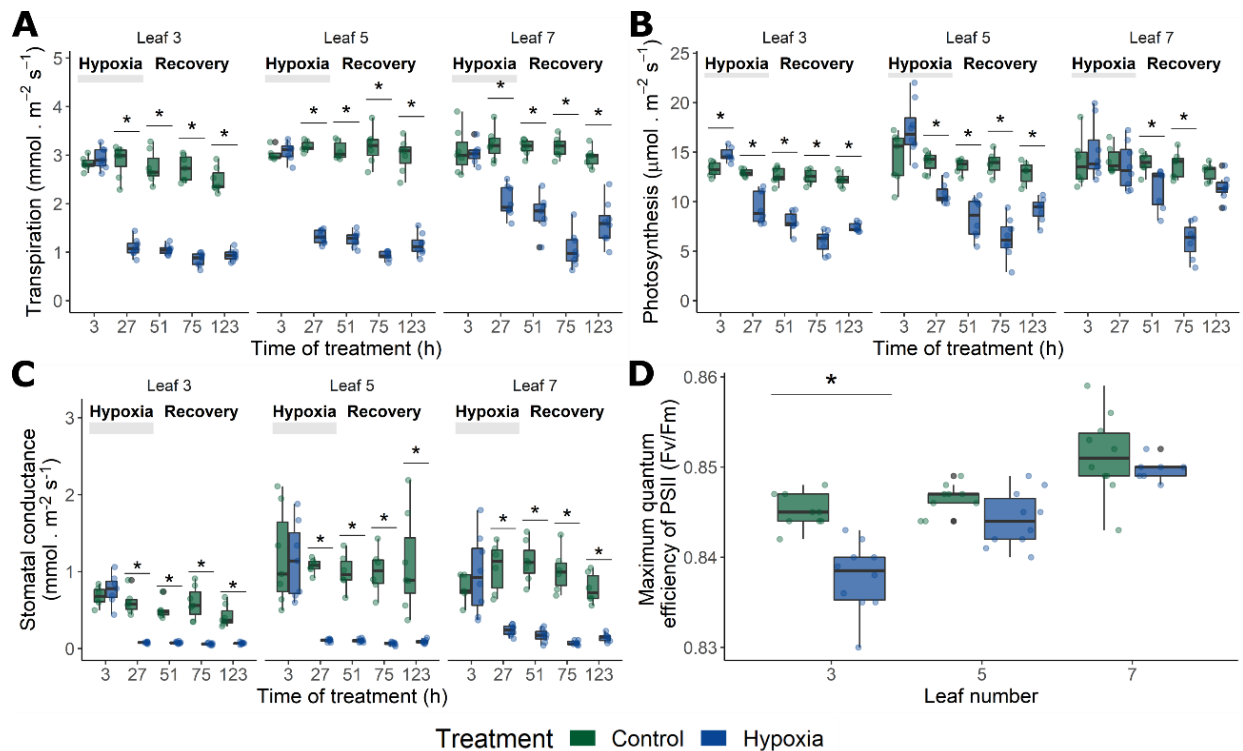
232 Figure 2: Physiological changes during waterlogging of tomato. (A) Canopy cover change determined from top view images (n =  
 233 10 – 11) after 96 h of waterlogging and 7 days of subsequent reoxygenation. (B) Total plant transpiration derived from real-time  
 234 lysimetry (n = 10 – 11) before, during and after a waterlogging treatment and relative to the initial canopy cover. (C) Total daily  
 235 plant transpiration integrated from (B). (D) Average daily plant CO<sub>2</sub> uptake (n = 6) during and after a waterlogging treatment.  
 236 Lines in (B) represent average transpiration rates +/- the confidence interval (90 %). Significant differences are indicated with an  
 237 asterisk ( $\alpha = 0.05$ ).

## 238 Leaf age determines physiological sensitivity towards root hypoxia

239 Given the effect of waterlogging on whole-plant performance, we wondered how leaves of different ages  
240 respond to waterlogging. Both leaf transpiration (Figure 3A) and leaf photosynthesis (Figure 3B) rate  
241 decreased throughout the treatment for all leaf age classes, but more rapidly in older leaves (Figure 3A –  
242 B). Recovery, especially for photosynthesis, was faster for young leaves during reoxygenation. The  
243 resilience of young leaves is not reflected by the plasticity of their stomatal conductance, which decreased  
244 drastically during waterlogging for all leaves and did not restore during reoxygenation. This suggests that  
245 recovery of photosynthesis in young leaves is largely independent of stomatal conductance (Figure 3C).

246 This discrepancy prompted us to quantify the maximum quantum efficiency of photosystem II (PSII;  $F_v/F_m$ ),  
247 which decreased significantly in older (leaf 3) and middle-aged leaves (leaf 5) after 48 h and 54 h (data not  
248 shown) respectively, but not in young leaves (leaf 7; Figure 3D). Collectively, these leaf-specific results  
249 suggest that older leaves suffer more from waterlogging, while recently emerged leaves are able to limit  
250 root hypoxia induced PSII damage. Ultimately, reduced transpiration and carbon assimilation during 48 h  
251 of root hypoxia led to a decline in leaf fresh and dry weight mainly for middle-aged and young leaves,  
252 indicative of growth reduction (Supporting Information Fig. S3).

253



254

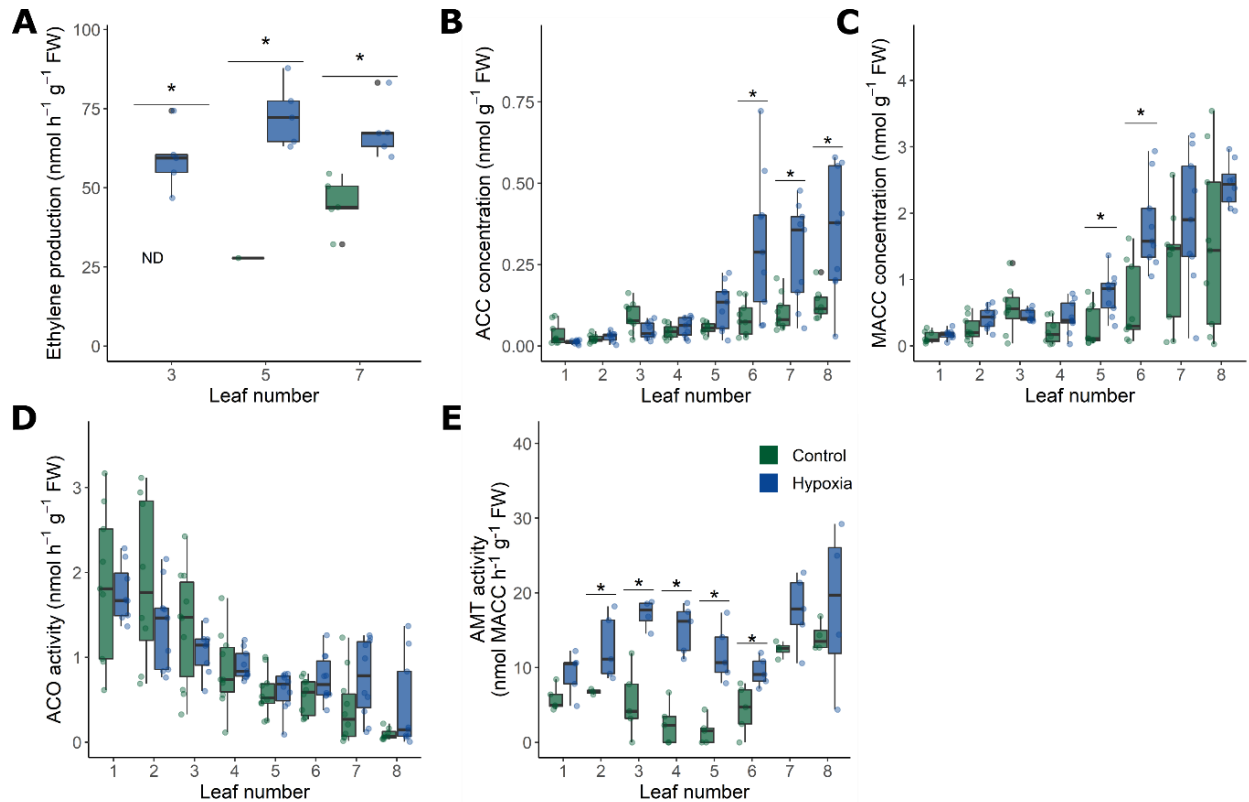
255 Figure 3: Leaf age-dependent changes of transpiration and photosynthesis during waterlogging and reoxygenation. Reduction of  
256 (A) leaf transpiration rate (B) leaf photosynthesis rate and (C) stomatal conductance, measured with an LCI photosynthesis system  
257 ( $n = 7 - 8$ ). (D) Maximum quantum efficiency of PSII after 48 h of waterlogging treatment ( $n = 10$ ). Significant differences are  
258 indicated with an asterisk ( $\alpha = 0.05$ ).

## 259 Ethylene biosynthesis is ontogenically triggered by waterlogging

260 Ethylene plays a major role in the epinastic response during waterlogging, but the ontogenic regulation  
261 of the ethylene metabolism has not yet been explored. Therefore, we investigated ethylene biosynthesis  
262 of leaves of different ages during waterlogging. We first quantified ethylene production of leaf petioles of  
263 different ages (Figure 4A) and found that 24 h of waterlogging significantly enhanced ethylene production  
264 in petioles of all leaf ages, but the response was higher in older (leaf 3) and middle-aged (leaf 5) leaves.

265 To further unravel this ontogenic relation, several key intermediates of the ethylene biosynthesis pathway  
266 were measured for leaves of different ages during waterlogging. Our analysis showed that levels of the  
267 ethylene precursor ACC and its primary conjugate MACC were higher in younger leaves, and increased  
268 after 24 h of root hypoxia (Figure 4B & C). On the other hand, the total *in vitro* ACO activity was higher in  
269 older leaves, and did not change significantly after the hypoxia treatment (Figure 4D & E). The *in vitro*  
270 AMT activity, however, was stimulated in older and middle-aged leaves (leaf 3 – 5) by the hypoxia  
271 treatment, while it remained at a high level in young leaves (leaf 7). Together, these data indicate a

272 complex ontogenic shift in the ACC metabolism. During waterlogging, ACC is transported from the roots  
 273 to the shoot, and is most likely converted into ethylene in older leaves due to a high ACO activity. In  
 274 contrast, the lower ACO and higher basal AMT activity in young leaves resulted in a lower ethylene  
 275 production rate, leading to ACC accumulation and conversion into MACC. The increase of AMT activity of  
 276 middle-aged leaves might limit ethylene production levels.

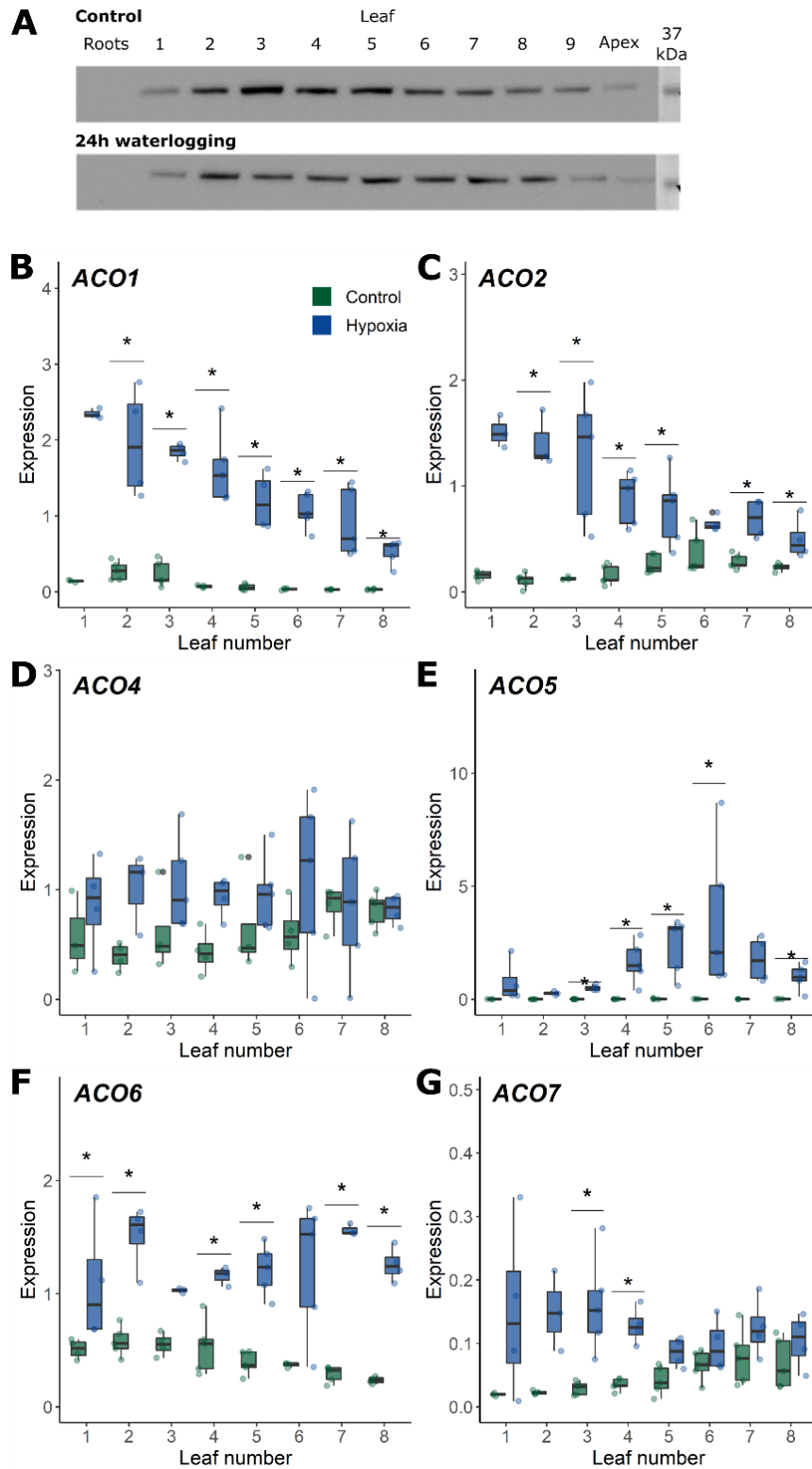


277  
 278 Figure 4: Ontogenic differentiation of ethylene biosynthesis during waterlogging. (A) Ethylene production of tomato petioles after  
 279 24 h of waterlogging (n = 5). (B – E) Changes in (B) the ethylene precursor ACC (n = 10), (C) the primary ACC conjugate MACC (n =  
 280 10), (D) enzyme activity of ACO (n = 10) and (E) enzyme activity of AMT (n = 5) after 24 h of waterlogging. Significant differences  
 281 are indicated with an asterisk ( $\alpha = 0.05$ ).

## 282 Waterlogging induces differential regulation of the ACO gene family

283 In order to unravel the differences in ethylene production observed in leaves of different ages, we  
 284 quantified total ACO protein abundance and the expression of several important ACO genes. Western blot  
 285 analysis confirmed an ontogenic trend in ACO abundance, but did not show any increase after the hypoxia  
 286 treatment (Figure 5A), matching the ACO *in vitro* activity (Figure 4D), with the exception of the oldest leaf  
 287 (leaf 1), which had a high *in vitro* ACO activity and a low ACO protein abundance (Figure 4D & Figure 5A).  
 288 Possibly, other ACO isoforms not detected by our antibody contribute to the ACO activity of leaf 1. A RT-

289 qPCR analysis showed clear diversification in the expression of the *ACO* gene family with respect to  
290 ontogeny and hypoxia stress (Figure 5B – G). The expression of different *ACOs* under control conditions  
291 strongly depended on leaf age, with a slightly higher expression of *ACO2* and *ACO7* in younger untreated  
292 leaves. However, during root hypoxia, several *ACO* isogenes showed a strong upregulation, especially in  
293 older leaves for *ACO1*, *ACO2* and *ACO7* and in middle-aged leaves for *ACO5* (Figure 5B – G), not leading to  
294 an increase in *ACO* protein abundance (Figure 5A), but possibly contributing to the higher ethylene  
295 production rate (Figure 4A).



296

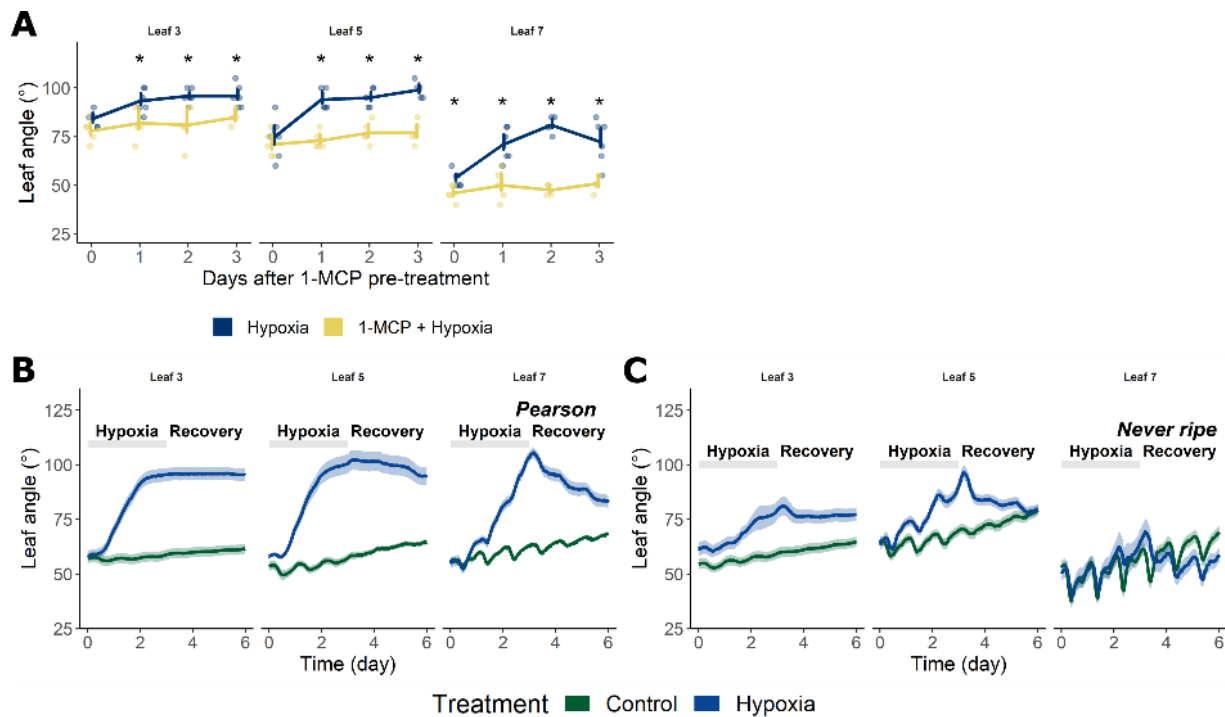
297 Figure 5: Effect of waterlogging on (A) the ACO abundance measured by western blotting (marker shows the 37 KDa protein size)

298 and the relative expression of tomato (B) *ACO1*, (C) *ACO2*, (D) *ACO4*, (E) *ACO5*, (F) *ACO6* and (G) *ACO7* in leaves of different

299 developmental stages and after 48 h of waterlogging (n = 5). Significant differences are indicated with an asterisk ( $\alpha = 0.05$ ).

## 300 Ethylene sensitivity steers the epinastic response and its recovery

301 The ontogenic discrepancy between the ethylene production and its genetic and metabolic regulation at  
302 the leaf level prompted us to investigate the role of ontogeny in ethylene responsiveness. Although we  
303 did not observe waterlogging induced changes in an *EBS::GUS* reporter line, GUS levels seemed to change  
304 slightly during development. In general, the intensity of the GUS signal decreased in older petioles  
305 (Supporting Information Fig. S6), similar to petiole ethylene production levels (Figure 4A). Next, we  
306 evaluated ethylene sensitivity during waterlogging using a 1-MCP treatment and the *Nr* mutant, a natural  
307 mutant of ethylene receptor 3 (SIETR3) (Chen et al., 2019; Hackett et al., 2000; Lanahan et al., 1994). Our  
308 results showed that a 1-MCP pre-treatment strongly inhibited waterlogging-induced epinasty for leaves  
309 of all ages (Figure 6A). Dynamic leaf angle data of the *Nr* mutant supported these results, showing a strong  
310 reduction of the epinastic curvature during root hypoxia, especially for young leaves, followed by a faster  
311 recovery (Figure 6B & C). Altogether, these data confirm that ethylene signaling is key for epinasty during  
312 root hypoxia, but also reveal that ethylene sensitivity is differentially regulated in leaves of different ages.



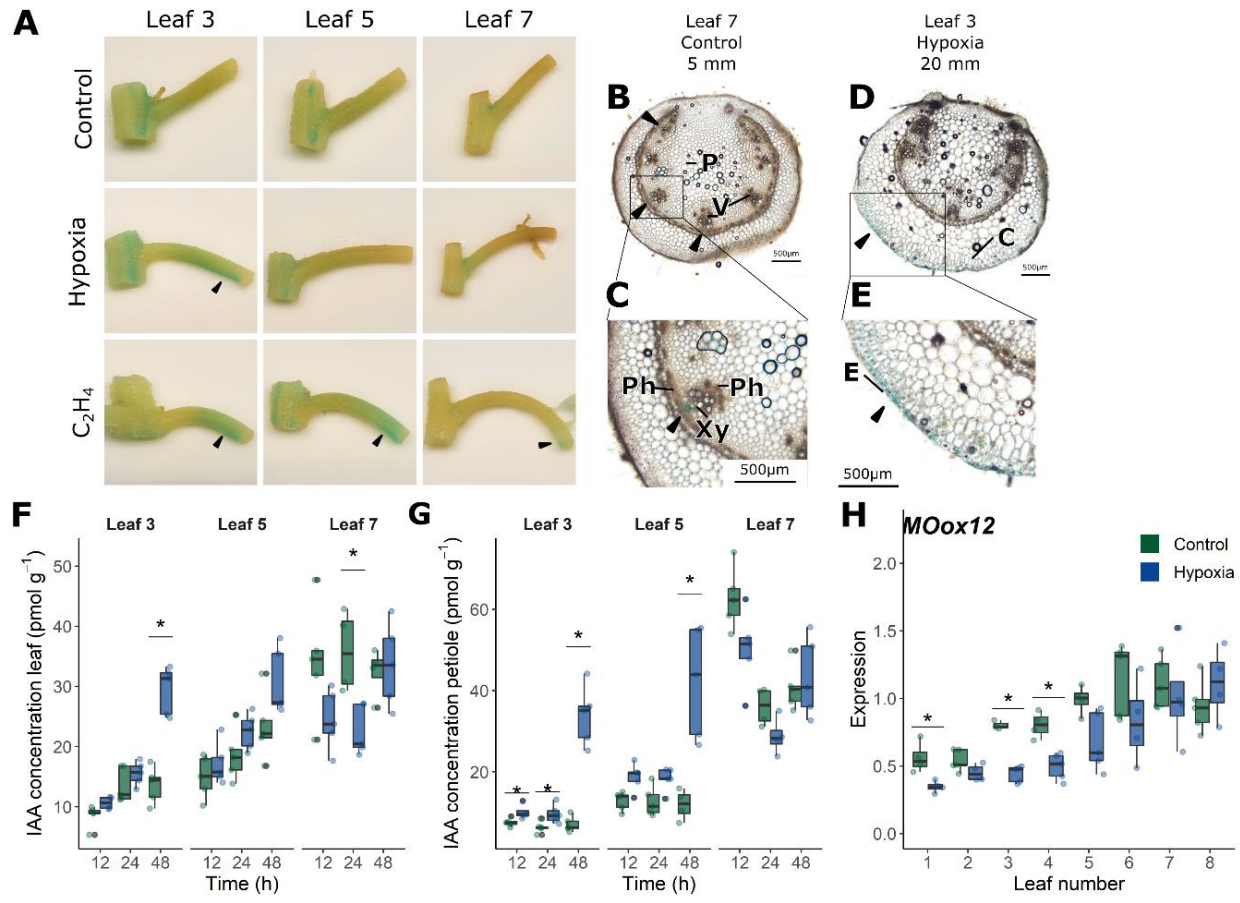
313  
314 Figure 6: Ethylene sensitivity of leaves of different ages during waterlogging. (A) Effect of a 1-MCP (1 ppm) pre-treatment on the  
315 epinastic curvature after 48 h of waterlogging (n = 5 – 6). Significant differences are indicated with an asterisk ( $\alpha = 0.05$ ). (C – D)  
316 Epinastic response to waterlogging in the (B) Pearson background and (C) the *Nr* mutant. Lines in (C – D) represent average leaf  
317 angles +/- the confidence interval (90%).



## 318 Waterlogging triggers auxin accumulation and responses in older leaves

319 Differentiation of ethylene biosynthesis and sensitivity might affect downstream regulation of epinasty  
320 through the auxin metabolism. To investigate auxin responses of petioles of different ages, we performed  
321 a histochemical analysis of a *DR5::GUS* reporter line (after 24 and 48 h of waterlogging) (Figure 7A &  
322 Supporting Information Fig. S7A). Auxin responses were generally more prevalent at the abaxial side of  
323 the petiole of old and mature leaves (leaf 3 – 5; Figure 7A), resembling the effect of an external ethylene  
324 treatment (Figure 7A). At the cellular level, GUS signals were stronger along the vascular tissue and the  
325 outer cell layers in petioles of young and middle-aged leaves under control conditions (Figure 7B – E). GUS  
326 staining in the parenchyma and collenchyma was also visible, but was mainly confined to abaxial cell layers  
327 of the petiole and the rachis during waterlogging (Figure 7D – E). These observations suggest that either  
328 local auxin production or its transport is augmented in the leaf petiole in an ontogenic way during  
329 waterlogging.

330 Hormone analysis confirmed that IAA levels increased significantly in older and middle-aged leaves and  
331 petioles, especially after 48 h of waterlogging (Figure 7F – G & Supporting Information Fig. S7). Young  
332 leaves and petioles already contained a higher IAA level under control conditions, which remained stable  
333 (or even gradually decreased) during waterlogging. The auxin precursors tryptophan (TRP) and tryptamine  
334 (TRA) decreased rapidly (12 h) in all leaves during the waterlogging treatment, while anthranilate (ANT)  
335 levels only declined in young leaves (Supporting Information Fig. S7C – E). In petioles, the concentration  
336 of TRP and IAA increased after 48 h of hypoxia. Collectively, these data indicate that auxin production is  
337 dampened in young leaves but elevated in older petioles during waterlogging. The main auxin catabolite  
338 oxIAA increased significantly in petioles of all leaf ages, suggesting root hypoxia induces auxin conjugation  
339 (Supporting Information Fig. S7F). Both in control and waterlogged conditions, this conjugation was more  
340 prominent in young leaves. While IAA levels increased in older leaves and petioles, the expression of a  
341 *YUCCA*-like *FLAVIN MONOOXYGENASE* (Solyc08g068160), an IAA biosynthesis gene, was partially  
342 downregulated in old and middle-aged leaves after 48 h of waterlogging (Figure 7H). In young leaves, on  
343 the other hand, the expression of this auxin biosynthesis gene did not differ between the treatments, in  
344 accordance with the actual IAA levels. The time lag between the major shift in auxin metabolism (48 h  
345 after treatment) and the onset of the actual epinastic response (within 12 h) is indicative of a more  
346 complex regulation of auxin homeostasis, and could result from rapid changes in IAA mobility.



347

348 Figure 7: Auxin responses and metabolism in tomato leaves and petioles after a waterlogging treatment. (A) *DR5::GUS* expression  
349 in tomato petioles of leaf 3, 5 and 7 after 48 h of waterlogging or overnight ethylene treatment (10 ppm). (B – E) *DR5::GUS*  
350 expression in the petiole of (B – C) leaf 7 in control conditions, localized in the vascular tissue (5 mm from the proximal end) and  
351 (D – E) leaf 3 after 48 h of waterlogging, localized in the abaxial collenchyma (20 mm from the proximal end). Arrows indicate  
352 regions with GUS staining (V = vascular bundle; P = parenchyma; C = collenchyma; Ph = phloem; Xy = xylem; E = epidermis). (F –  
353 G) Auxin (IAA) levels in tomato (F) leaves and (G) petioles of different ages during the waterlogging treatment (n = 5). (H) Gene  
354 expression of an IAA biosynthesis gene *FLAVIN MONOOXYGENASE* in tomato leaves after 48 h of waterlogging (n = 5). Significant  
355 differences are indicated with an asterisk ( $\alpha = 0.05$ ).

### 356 Auxin transport is ontogenically gated during waterlogging

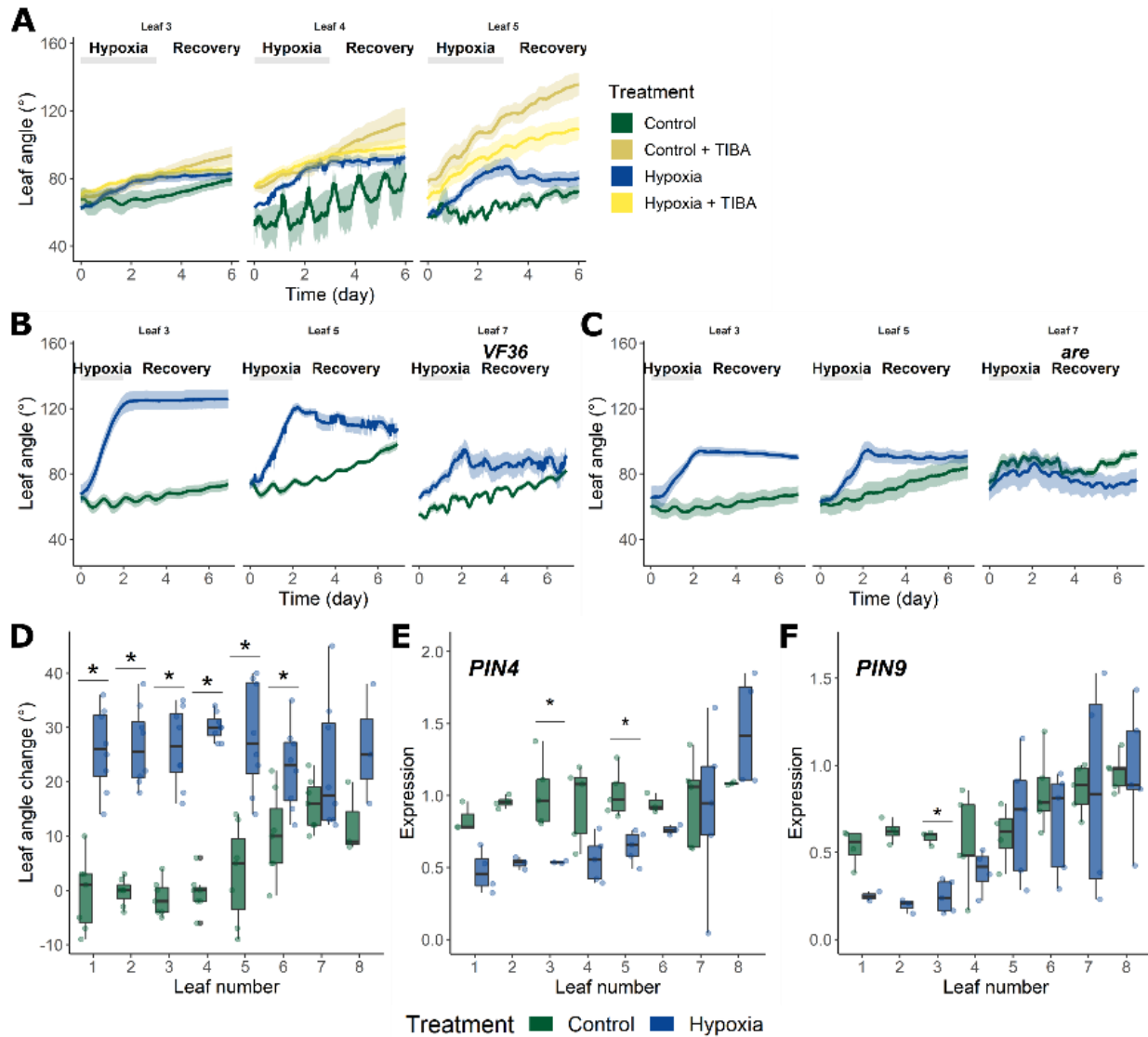
357 Auxin transport is known to regulate cellular development and elongation, but its role in the ontogenic  
358 control of leaf epinasty during waterlogging is unknown. A foliar treatment with TIBA, an inhibitor of polar  
359 auxin transport, resulted in a reduction of the epinastic response during waterlogging in older and middle-  
360 aged leaves (Supporting Information Fig. S8). However, the TIBA application itself also caused downwards  
361 bending and curling of control leaves. A local petiole application of TIBA lanolin paste confirmed that TIBA  
362 stimulates leaf epinasty, irrespective of the waterlogging treatment (Figure 8A). Furthermore, young  
363 leaves continued to bend down after the TIBA application, even during the reoxygenation phase.

364 Intriguingly, epinastic bending of older and middle-aged leaves treated with TIBA stabilized during this  
365 phase. Besides the effect on leaf bending, inhibition of auxin export by TIBA also caused major leaf curling  
366 and changes in petiole morphology in young leaves, demonstrating the importance of polar auxin  
367 transport in leaf development (Supporting Information Fig. S9). Depending on leaf age, TIBA led to an  
368 accumulation of *DR5::GUS* expression upstream or downstream of the site of application of the lanolin  
369 paste. In young leaves, there was an increased GUS signal at the distal side, while in old leaves it was at  
370 the abaxial side of the petiole base (Supporting Information Fig. S10).

371 The *are* mutant, characterized by a reduction of anthocyanins and their flavonol precursors, has a higher  
372 auxin flow (Maloney et al., 2014). This increased auxin flux in the *are* mutant reduced the intensity of the  
373 epinastic curvature (Figure 8B & C), corroborating the role of IAA transport in the waterlogging response.  
374 We evaluated the anthocyanin content in leaves, showing no alterations after 48 h of waterlogging  
375 (Supporting Information Method S2; Supporting Information Fig. S11). However, existing ontogenic  
376 differences might already interfere with auxin mobility.

377 Besides flavonols, auxin fluxes are predominantly controlled by PIN-formed (PIN) transporters. One of the  
378 exporters, PIN4, is strongly expressed in leaves (Pattison & Catalá, 2012). A *PIN4-RNAi* line showed a  
379 relatively normal epinastic movement during waterlogging (Figure 8D), but was already constitutively and  
380 mildly epinastic in old and mature leaves. These leaves also showed a decline in the expression of *PIN4*  
381 and another efflux carrier gene (*PIN9*) after 48 h of waterlogging (Figure 8E & F). Altogether, these results  
382 imply that auxin transport is impeded in old and mature leaves during waterlogging, in turn supporting  
383 IAA accumulation (Figure 7F) and signaling (Figure 7A) in these leaves.

384



385

386 Figure 8: Ontogenic auxin transport in tomato leaves and petioles after a waterlogging treatment. (A) Effect of petiolar TIBA  
 387 application (1 %) on leaf angle dynamics during waterlogging (n = 5 – 9). (B – C) Leaf angle change in the *are* mutant and its  
 388 background VF36 during 48 h of waterlogging and reoxygenation (n = 5 – 10). (D) Epinastic response of a *PIN4-RNAi* line after 48  
 389 h of waterlogging (n = 7 – 8). (E – F) Gene expression of (E) *PIN4* and (F) *PIN9* transporters in tomato leaves after 48 h of  
 390 waterlogging (n = 5). Lines in (D – E) represent average leaf angles +/- the 90 % confidence interval. Significant differences are  
 391 indicated with an asterisk ( $\alpha = 0.05$ ).

## 392 Discussion

### 393 Leaf ontogeny defines epinastic curvature and recovery during waterlogging

394 Throughout development, leaves undergo several morphological, physiological and biochemical changes  
 395 (Efroni et al., 2008). This process leads to the dynamic regulation of growth and determines the potential

396 to respond to environmental cues (Rankenberg et al., 2021). We showed that one of these age-dependent  
397 responses is waterlogging-induced leaf epinasty, allowing young growing leaves to quickly re-adjust their  
398 posture after waterlogging.

399 This age-related plasticity has been described before for flooding-induced petiole elongation in *R. palustris*  
400 (Groeneveld & Voeselek, 2003), *R. pygmaeus* (Horton, 1992) and rice (*Oryza sativa*) (Alpuerto et al.,  
401 2022). In tomato, this age-related response seems to be regulated by cellular expansion during leaf growth  
402 (Figure 1). Waterlogging caused epinasty by reducing petiole and epidermal cell elongation of young  
403 leaves, mainly at the abaxial side, while promoting elongation in mature leaves, mainly at the adaxial side.  
404 This developmental dependency of cell and tissue elongation was also demonstrated for rice plants that  
405 need to reach a certain developmental stage before flooding can induce internode elongation (Ayano et  
406 al., 2014). In the monocot *Festuca arundinacea*, leaf elongation rates also increase with age (Xu et al.,  
407 2016).

#### 408 Young leaves retain a higher physiological plasticity during waterlogging

409 The effect of waterlogging on tomato physiology has been described without accounting for leaf ontogeny  
410 (Bradford & Hsiao, 1982; Else et al., 2009). We have shown that a short deprivation of oxygen in the root  
411 zone determines subsequent plant survival during reoxygenation (Figure 2), mainly depending on  
412 restoration of transpiration and photosynthesis in young leaves (Figure 3A – B). During drought stress in  
413 cotton (Jordan et al., 1975) and grapevine (Hopper et al., 2014), young leaves also showed higher  
414 resilience.

415 The plasticity of young leaves in terms of NPQ has been described as a possible protective mechanism  
416 against photoinhibition in Arabidopsis (Bielczynski et al., 2017). Young tomato leaves also seem capable  
417 of preventing these deleterious effects, as their PSII maximal quantum efficiency was unaffected by  
418 waterlogging in contrast to older leaves (Figure 3D). However, not every stress condition influences leaf  
419 performance in the same age-dependent way. Young expanding coffee leaves, for example, seem to be  
420 more prone to heat-induced reduction of both photosynthesis and stomatal closure (Marias et al., 2017).

#### 421 Leaf ontogeny defines the transcriptional regulation of *ACO* and the biosynthesis of ethylene

422 We have shown that both ethylene metabolism and *ACO* expression are ontogenically regulated in tomato  
423 (Figure 4 & Figure 5). Under control conditions, young tomato leaves harbor more ACC and produce a  
424 higher amount of ethylene, similar to young Arabidopsis leaves (Berens et al., 2019). Ontogenic regulation  
425 of *ACS* gene expression might contribute to this ACC gradient, as was shown before for maize (Young et

426 al., 2004) and white clover (*Trifolium repens*) leaves (Murray & Mcmanus, 2005). During waterlogging,  
427 more ACC enters the leaves by xylem-mediated transport from the roots (Bradford & Yang, 1980a).

428 In white clover, ACC content and ethylene production of different leaves has been linked to differences in  
429 ACO activity (Chen & McManus, 2006; Hunter et al., 1999). In Arabidopsis, *AtACO1* is upregulated in roots  
430 during short term waterlogging (Hsu et al., 2011), and in both roots and shoot during long term  
431 waterlogging (Ventura et al., 2020) or hypoxia (Hsu et al., 2011). Our own transcriptional analysis showed  
432 that *SIACO5*, belonging to the same clade as *AtACO1* (Houben & Van de Poel, 2019), is strongly  
433 upregulated in an ontogenic way, with the highest expression in mature and younger leaves (Figure 5).  
434 The closest ortholog to *AtACO5*, the only ACO previously linked to leaf bending (Rauf et al., 2013), is  
435 *SIACO7* (Houben & Van de Poel, 2019) and is predominantly upregulated in older and mature leaves. This  
436 also counts for *SIACO1*, explaining the reduced epinastic bending in older leaves of its antisense line during  
437 waterlogging in tomato (English et al., 1995). The differential expression of ACO genes by age and  
438 waterlogging does not reflect in differences in ACO protein abundance nor *in vitro* activity, hinting towards  
439 a possible post-translational regulation ACO.

440 This indicates that differentiation of the ACOs provides a mechanism to control ethylene-regulated stress  
441 responses in a tissue- and age-specific way (Figure 9). In tomato, this leads to higher ethylene production  
442 in younger leaves during control and waterlogging conditions (Jackson & Campbell, 1976), but not during  
443 drought stress (Abou Hadid et al., 1986). In petioles, the increased ethylene production is relatively higher  
444 for older and mature leaves (Figure 4A). One mechanism that could further contribute is conjugation of  
445 ACC (Pattyn et al., 2021). Indeed, MACC accumulation is higher in young leaves, probably through higher  
446 basal AMT activity (Figure 4E). In contrast, old leaves activate AMT during waterlogging without a  
447 detectable change in MACC content.

#### 448 Leaf plasticity is determined by ontogenic changes in ethylene sensitivity

449 Leaf plasticity towards stress can also be explained by developmental differences in ethylene sensitivity  
450 and signaling (Edelman & Jones, 2014; Kanojia et al., 2020; Kim et al., 2009; Li et al., 2013). In  
451 submergence-tolerant rice, ethylene sensitivity is developmentally controlled by differential regulation of  
452 *SUBMERGENCE1A* (*SUB1A*) dependent pathways, leading to a stronger growth reduction in young leaves  
453 (Alpuerto et al., 2022). In contrast, young rosette leaves of Arabidopsis seem to be more hyponastic after  
454 application of exogenous ethylene (Vandenbussche et al., 2003) and during waterlogging (Rauf et al.,  
455 2013). Similar differences in ethylene sensitivity could dampen leaf epinasty in young leaves during

456 waterlogging (Figure 1B). This age-dependent sensitivity to ethylene and the corresponding epinastic  
457 response have also been reported for other *Solanaceae* species (Edelman & Jones, 2014).

458 A 1-MCP treatment prevented waterlogging-induced epinastic bending of all leaves (Figure 6A), indicating  
459 that ethylene signaling is crucial for epinastic bending (Figure 9). The *Nr* mutation also inhibits epinastic  
460 responses (Barry et al., 2005; Lanahan et al., 1994). The residual epinastic curvature observed in older and  
461 mature leaves of the *Nr* mutant during waterlogging (Figure 6C – D) indicates that the ethylene signal still  
462 gets partially transduced by other receptors (Chen et al., 2019; Hackett et al., 2000; Lanahan et al., 1994).

### 463 Elevated auxin levels in mature tomato leaves contribute to epinasty during waterlogging

464 Ethylene sensitivity is often intertwined with auxin homeostasis, signaling and transport (Muday et al.,  
465 2012), which is developmentally regulated in *Arabidopsis* (Ljung et al., 2002). In general, young leaves are  
466 biosynthetically active and rely on different modes of auxin transport, leading to ontogenic differences in  
467 auxin sensitivity (Ljung et al., 2002). As a result, both auxin depletion and accumulation might yield leaf-  
468 specific responses. The reduction of auxin levels during tomato leaf ageing (Figure 7F – G) could explain  
469 developmental differences in leaf bending (Figure 1 D&F). However, the role of auxins in developmentally  
470 steered elongation might be more complex. In rice, for example, submergence-induced leaf elongation is  
471 less prominent in mature leaves, despite the higher accumulation of auxins (Alpuerto et al., 2022). On the  
472 other hand, rice coleoptile elongation under submergence is directly related to an increased auxin content  
473 (Nghie et al., 2021).

474 In tomato, waterlogging elevates auxin levels in mature leaves and decreases auxin precursors (TRP and  
475 TRA) in older leaves (Figure 7F – G; Supporting Information Fig. S7). This indicates there is enhanced IAA  
476 synthesis during waterlogging, despite one *YUCCA* homolog not being upregulated (Figure 7H). Another  
477 mechanism that might contribute to differential age-related auxin levels is conjugation. In *Arabidopsis*,  
478 the glucosyltransferase *UGT74D1* is mainly expressed in young leaves, and overexpression of *UGT74D1*  
479 results in increased IAA levels and ultimately in less erect leaves (Jin et al., 2021). Oxidation of IAA into  
480 the inactive oxIAA in young tomato petioles (Supporting Information Fig. S7) might provide an additional  
481 feedback mechanism to control auxin homeostasis.

482 Besides IAA synthesis and breakdown, reduced auxin export by PIN transporters, reflected by a reduced  
483 expression of *PIN4* and *PIN9* (Figure 8E – F), possibly contributes to IAA accumulation in older leaves  
484 during waterlogging (Figure 7F – G; Figure 9). Accumulation of auxins due to tissue-specific inhibition of  
485 IAA transport seems likely, as the *PIN4* RNAi line (Figure 8D) and an application of the auxin export

486 inhibitor TIBA (Figure 8A) both showed epinasty, irrespective of a waterlogging treatment and leaf age. A  
487 similar mechanism has been described in the *Atmdr1* mutant of Arabidopsis, characterized by inhibition  
488 of auxin transport and leaf epinasty (Noh et al., 2001), and after disrupting the auxin balance in flooded  
489 *R. palustris* (Cox et al., 2004). IAA accumulation does not occur in young leaves during waterlogging (Figure  
490 8D), characterized by high *PIN4* and *PIN9* expression (Figure 8E – F), possibly sustaining auxin efflux (Figure  
491 9).

492 Auxin transporters can be inhibited by flavonols (Kuhn et al., 2017). Flavonol overproducing mutants of  
493 Arabidopsis display a hyponastic phenotype, albeit in the leaf blade itself (Kuhn et al., 2011). In contrast,  
494 enhanced auxin transport in the *are* mutant in tomato reduces auxin accumulation (Maloney et al., 2014),  
495 which leads to a dampened epinastic response after waterlogging (Figure 6 & Figure 8). However, leaf  
496 epinasty in the *are* mutant can also be affected by changes in ROS metabolism and signaling.

497 Previously, it was proposed that auxins are redistributed towards the fast elongating side of the petiole  
498 (adaxial) during ethylene-induced epinasty in tomato (Lee et al., 2008) or during thermonasty (abaxial) in  
499 Arabidopsis (Park et al., 2019). In contrast, we observed a slight overall increase in DR5::GUS activity  
500 mostly at the abaxial side of older petioles during waterlogging.

501 Collectively, our data suggest that auxin accumulation by enhanced IAA production and reduced IAA  
502 export at the petiole base stimulates leaf epinasty in mature tomato leaves during waterlogging, while  
503 auxin transport is better sustained in young leaves, leading to stable IAA levels and thus a higher  
504 morphological plasticity during waterlogging (Figure 10).

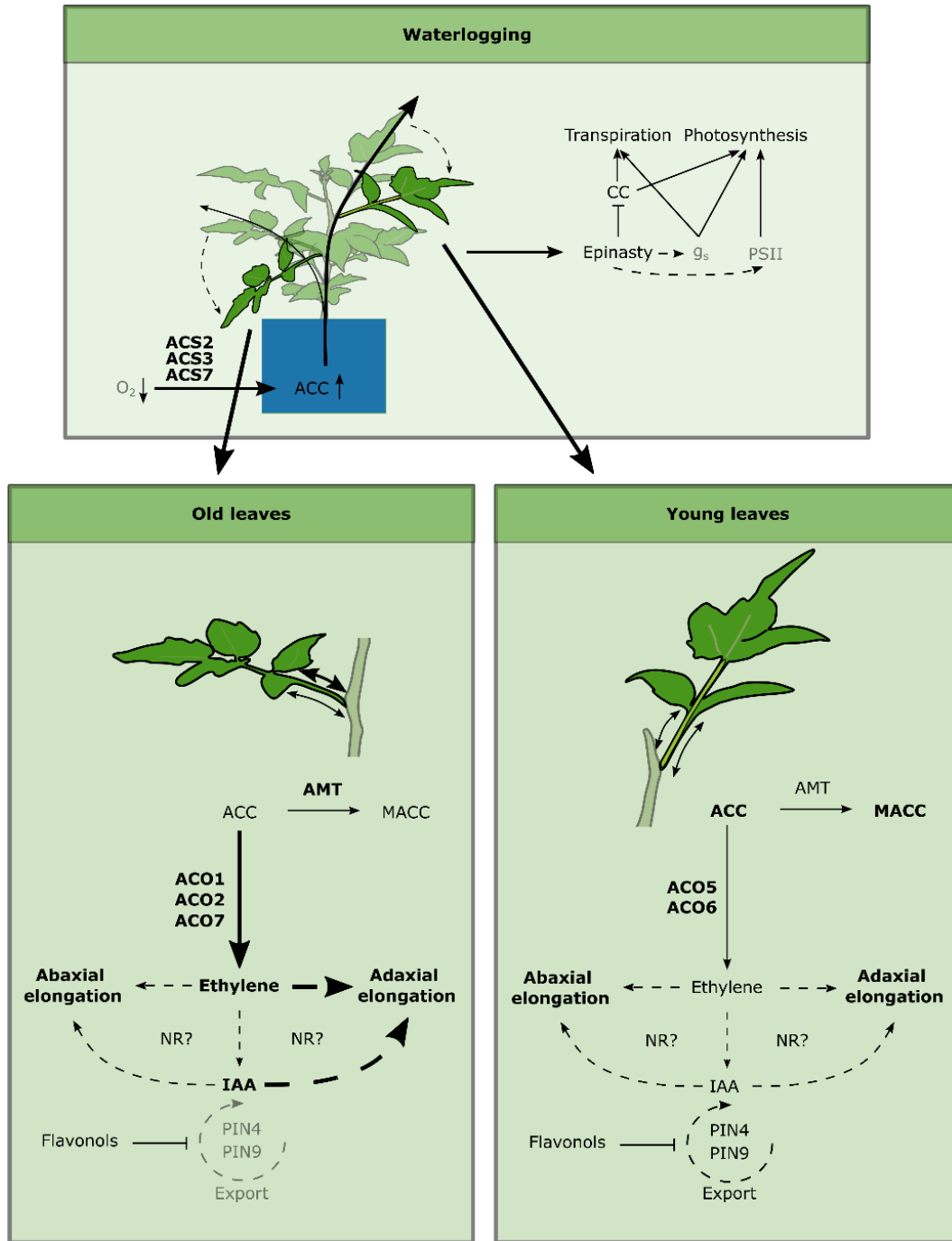
### 505 Ontogeny as an interface for regulating epinasty by ethylene and auxin crosstalk?

506 The concerted action of ethylene and auxins sets the scene for normal plant development (Van de Poel et  
507 al., 2015) and is often fine-tuned in a tissue-specific way (Muday et al., 2012), providing a framework for  
508 ontogenic regulation. Ethylene can either directly influence cell cycling and elongation (Dubois et al., 2018;  
509 Pierik et al., 2006) or change auxin homeostasis through modification of IAA production or transport. This  
510 dual action of ethylene could regulate the epinastic response in tomato, in spite of early reports on auxin-  
511 induced ethylene production regulating differential elongation in tomato petioles (Kazemi & Kefford,  
512 1974; Stewart & Freebairn, 1969).

513 The auxin insensitive tomato mutant *diageotropica* (*dgt*) displays an epinastic response to both  
514 exogenous ethylene (Ursin & Bradford, 1989b) and waterlogging (Bradford & Yang, 1980), suggesting  
515 epinasty is primarily regulated by ethylene. On the other hand, reduction of ethylene signaling in the *Nr*



516 mutant potentially affects cell elongation, but also enhances auxin transport in the hypocotyl, but not in  
517 roots (Negi et al., 2010). As a result, reduced epinasty in the *Nr* mutant might be the result of reduced  
518 ethylene sensitivity, but also of enhanced auxin transport (Figure 6; Negi et al., 2010) and disrupted auxin  
519 signaling (Lin et al., 2008). Altered ethylene signaling in this mutant causes development-dependent  
520 petiole bending (Figure 6), which might be due to ethylene and auxin responses. This is not surprising,  
521 given that ethylene and auxin signaling are integrated in regulatory hubs, such as *S//AA3* (Chaabouni et  
522 al., 2009) and *S//ERF.B3* (Liu et al., 2018) to establish tissue specific responses to both hormones. *S//AA3*, a  
523 positive regulator of auxin responses in tomato petioles, is differentially expressed in petioles after  
524 ethylene treatment (Chaabouni et al., 2009), suggesting that it acts as an ethylene-mediated activator of  
525 auxin responses. The actual mechanism integrating ethylene and auxin responses in the petiole of tomato  
526 remains to be discovered.



527

528 Figure 9: Schematic overview of the ontogenic differentiation of the epinastic response during waterlogging in tomato. Low

529 oxygen conditions in the roots stimulate ACC production, at least by ACS2, ACS3 and ACS7 (Olson et al., 1995; Shiu et al., 1998),

530 leading to accumulation of ACC in the root zone. This ACC is transported to the shoot, where it is distributed mainly towards

531 young sink leaves, capable of effectively conjugating ACC into the inactive MACC. Differential expression of the ACO gene family

532 allows for intricate regulation of local ethylene production, which is stimulated mainly in older leaves. Ethylene itself activates

533 cellular elongation, in part through NR signaling and the regulation of local auxin levels. Auxin export is inhibited in old leaves by

534 reduced expression of *PIN4* and *PIN9* auxin exporters, promoting its accumulation at the base of the petiole. This in turn disrupts

535 local elongation dynamics within the petiole, leading to a relatively higher adaxial cell elongation and ultimately epinastic bending  
536 (and reduction in canopy cover, CC). In young leaves, auxin export capacity is sustained and hormonal balances are faster  
537 restored, leading to enhanced morphological plasticity and resilience during waterlogging and recovery. Most likely, other factors  
538 come into play to define the proper transduction of polar responsiveness within the petiole, as inhibition of auxin export from  
539 the leaf alone (by TIBA) evokes specific secondary and age-related responses regarding leaf positioning, independent of  
540 waterlogging-induced epinasty.

## 541 **Acknowledgements**

542 We thank the KU Leuven Greenhouse Core Facility for assistance in plant cultivation and Veerle Verdoodt  
543 for performing the ACC, MACC and ACO measurements. This work was funded by the Research  
544 Foundation Flanders with a FWO PhD fellowship (11C4319N; 1150822N; 1502121N ) to BG, JP and PM  
545 respectively, and a FWO research grant (G092419N) to BVDP; by a KU Leuven research grant (C14/18/056)  
546 to BVDP and a PhD-back-up grant (DB/17/007/BM) to BG. This work was also established in the framework  
547 of the RoxyCost action of the EU (CA18210).

## 548 **Author contribution**

549 BG and BVdP designed the experiments, JP performed the RT-qPCR analyses and AMT activity assay, KVdB  
550 visualized and quantified cellular and macroscopic elongation of the petiole, VE assisted with physiological  
551 measurements, PM generated the EBS::GUS-GFP reporter line, ON supervised and designed the UHPLC-  
552 ESI-MS/MS protocol for auxin quantification, BG performed the experiments and analyzed the data, BG  
553 and BvDP wrote the manuscript. All authors read and approved the manuscript.

## 554 Supporting Information

555 Supporting Information Method S1: Cloning and plant transformation

556 Supporting Information Method S2: Anthocyanin extraction

557 Supporting Information Method S3: Differential cell elongation of the abaxial – adaxial petiole side

558 Supporting Information Table S1: Primers used for the qRT-PCR in this study

559 Supporting Information Table S2: Primers used for the tomato transformation in this study

560 Supporting Information Fig. S1: Petiole morphology and anatomy of the different leaves of tomato  
561 plants in the eighth leaf stage.

562 Supporting Information Fig. S2: Daily transpiration of tomato during and after a waterlogging treatment  
563 of 96 h.

564 Supporting Information Fig. S3: Effect of waterlogging (48 h) on biomass production in leaves of  
565 different ages.

566 Supporting Information Fig. S4: Effect of waterlogging (96 h) on biomass production in leaves of  
567 different ages.

568 Supporting Information Fig. S5: Petiole ethylene production after sampling.

569 Supporting Information Fig. S6: GUS expression in petioles of different ages in an *EBS::GUS* reporter line.

570 Supporting Information Fig. S7: Auxin responses and biosynthesis in leaves and petioles of different  
571 ages.

572 Supporting Information Fig. S8: Effect of inhibition of auxin transport (TIBA) on leaf epinasty during  
573 waterlogging.

574 Supporting Information Fig. S9: Morphological effects of a local TIBA application with lanolin paste on  
575 the petiole.

576 Supporting Information Fig. S10: DR5::GUS staining pattern in petioles treated with a 0.5 – 1 cm ring of  
577 TIBA in lanolin paste at the petiole base.

578 Supporting Information Fig. S11: Concentration of anthocyanins, natural inhibitors of auxin flows, in the  
579 different leaves.

580

581

## 582 References

- 583 Abou Hadid, A. F., El-Beltagy, A. S., Smith, A. R., & Hall, M. A. (1986). The influence of leaf position and age  
584 upon the production of stress ethylene in tomatoes. In *Acta Horticulturae* (Vol. 190, pp. 397–404).
- 585 Alpuerto, J. B., Fukuda, M., Li, S., Hussain, R. M. F., Sakane, K., & Fukao, T. (2022). The submergence  
586 tolerance regulator SUB1A differentially coordinates molecular adaptation to submergence in  
587 mature and growing leaves of rice (*Oryza sativa* L.). *The Plant Journal : For Cell and Molecular Biology*,  
588 *110*(1), 71–87. <https://doi.org/10.1111/tpj.15654>
- 589 Ayano, M., Kani, T., Kojima, M., Sakakibara, H., Kitaoka, T., Kuroha, T., Angeles-Shim, R. B., Kitano, H.,  
590 Nagai, K., & Ashikari, M. (2014). Gibberellin biosynthesis and signal transduction is essential for  
591 internode elongation in deepwater rice. *Plant Cell and Environment*, *37*(10), 2313–2324.  
592 <https://doi.org/10.1111/pce.12377>
- 593 Barry, C. S., McQuinn, R. P., Thompson, A. J., Seymour, G. B., Grierson, D., & Giovannoni, J. J. (2005).  
594 Ethylene insensitivity conferred by the Green-ripe and Never-ripe 2 ripening mutants of tomato.  
595 *Plant Physiology*, *138*(1), 267–275. <https://doi.org/10.1104/pp.104.057745>
- 596 Berens, M. L., Wolinska, K. W., Spaepen, S., Ziegler, J., Nobori, T., Nair, A., Krüler, V., Winkelmüller, T. M.,  
597 Wang, Y., Mine, A., Becker, D., Garrido-Oter, R., Schulze-Lefert, P., & Tsuda, K. (2019). Balancing  
598 trade-offs between biotic and abiotic stress responses through leaf age-dependent variation in stress  
599 hormone cross-talk. *Proceedings of the National Academy of Sciences of the United States of*  
600 *America*, *116*(6), 2364–2373. <https://doi.org/10.1073/pnas.1817233116>
- 601 Bielczynski, L. W., Łacki, M. K., Hoefnagels, I., Gambin, A., & Croce, R. (2017). Leaf and Plant Age Affects  
602 Photosynthetic Performance and Photoprotective Capacity. *Plant Physiology*, *175*(4), 1634–1648.  
603 <https://doi.org/10.1104/pp.17.00904>
- 604 Blakeslee, J. J., & Murphy, A. S. (2016). *Microscopic and Biochemical Visualization of Auxins in Plant Tissues*  
605 (Vol. 1398, pp. 37–53). [https://doi.org/10.1007/978-1-4939-3356-3\\_5](https://doi.org/10.1007/978-1-4939-3356-3_5)
- 606 Bradford, K. J., & Hsiao, T. C. (1982). Stomatal Behavior and Water Relations of Waterlogged Tomato  
607 Plants. *Plant Physiology*, *70*(5), 1508–1513. <https://doi.org/10.1104/pp.70.5.1508>
- 608 Bradford, K. J., & Yang, S. F. (1980a). Xylem Transport of 1-Aminocyclopropane-1-carboxylic Acid, an  
609 Ethylene Precursor, in Waterlogged Tomato Plants. *Plant Physiology*, *65*(2), 322–326.

- 610 <https://doi.org/10.1104/pp.65.2.322>
- 611 Bradford, K. J., & Yang, S. F. (1980b). Stress-induced Ethylene Production in the Ethylene-requiring Tomato  
612 Mutant Diageotropica. *Plant Physiology*, *65*(2), 327–330. <https://doi.org/10.1104/pp.65.2.327>
- 613 Bulens, I., Van de Poel, B., Hertog, M. L. A. T. M., De Proft, M. P., Geeraerd, A. H., & Nicolaï, B. M. (2011).  
614 Protocol: An updated integrated methodology for analysis of metabolites and enzyme activities of  
615 ethylene biosynthesis. *Plant Methods*, *7*(1), 1–10. <https://doi.org/10.1186/1746-4811-7-17>
- 616 Chaabouni, S., Jones, B., Delalande, C., Wang, H., Li, Z., Mila, I., Frasse, P., Latché, A., Pech, J.-C. C., &  
617 Bouzayen, M. (2009). SI-IAA3, a tomato Aux/IAA at the crossroads of auxin and ethylene signalling  
618 involved in differential growth. *Journal of Experimental Botany*, *60*(4), 1349–1362.  
619 <https://doi.org/10.1093/jxb/erp009>
- 620 Chen, B. C.-M., & McManus, M. T. (2006). Expression of 1-aminocyclopropane-1-carboxylate (ACC)  
621 oxidase genes during the development of vegetative tissues in white clover (*Trifolium repens* L.) is  
622 regulated by ontological cues. *Plant Molecular Biology*, *60*(3), 451–467.  
623 <https://doi.org/10.1007/s11103-005-4813-3>
- 624 Chen, Y., Rofidal, V., Hem, S., Gil, J., Nosarzewska, J., Berger, N., Demolombe, V., Bouzayen, M., Azhar, B.  
625 J., Shakeel, S. N., Schaller, G. E., Binder, B. M., Santoni, V., & Chervin, C. (2019). Targeted Proteomics  
626 Allows Quantification of Ethylene Receptors and Reveals SIETR3 Accumulation in Never-Ripe  
627 Tomatoes. *Frontiers in Plant Science*, *10*(August), 1–10. <https://doi.org/10.3389/fpls.2019.01054>
- 628 Cox, M. C. H., Benschop, J. J., Vreeburg, R. A. M., Wagemaker, C. A. M., Moritz, T., Peeters, A. J. M., &  
629 Voeselek, L. A. C. J. (2004). The roles of ethylene, auxin, abscisic acid, and gibberellin in the  
630 hyponastic growth of submerged *Rumex palustris* petioles. *Plant Physiology*, *136*(2), 2948–2960;  
631 discussion 3001. <https://doi.org/10.1104/pp.104.049197>
- 632 Cox, M. C. H., Millenaar, F. F., Van Berkel, Y. E. M. D. J., Peeters, A. J. M., & Voeselek, L. A. C. J. (2003).  
633 Plant movement. Submergence-induced petiole elongation in *Rumex palustris* depends on  
634 hyponastic growth. *Plant Physiology*, *132*(May), 282–291. <https://doi.org/10.1104/pp.102.014548>
- 635 Doubt, S. L. (1917). The Response of Plants to Illuminating Gas. *Botanical Gazette*, *63*(3), 209–224.
- 636 Dubois, M., Van den Broeck, L., & Inzé, D. (2018). The Pivotal Role of Ethylene in Plant Growth. *Trends in*  
637 *Plant Science*, *23*(4), 311–323. <https://doi.org/10.1016/j.tplants.2018.01.003>

- 638 Edelman, N. F., & Jones, M. L. (2014). Evaluating ethylene sensitivity within the family Solanaceae at  
639 different developmental stages. *HortScience*, 49(5), 628–636.  
640 <https://doi.org/10.21273/hortsci.49.5.628>
- 641 Efroni, I., Blum, E., Goldshmidt, A., & Eshed, Y. (2008). A protracted and dynamic maturation schedule  
642 underlies Arabidopsis leaf development. *Plant Cell*, 20(9), 2293–2306.  
643 <https://doi.org/10.1105/tpc.107.057521>
- 644 Else, M. A., Janowiak, F., Atkinson, C. J., & Jackson, M. B. (2009). Root signals and stomatal closure in  
645 relation to photosynthesis, chlorophyll a fluorescence and adventitious rooting of flooded tomato  
646 plants. *Annals of Botany*, 103(2), 313–323. <https://doi.org/10.1093/aob/mcn208>
- 647 English, P. J., Lycett, G. W., Roberts, J. A., & Jackson, M. B. (1995). Increased 1-Aminocyclopropane-1-  
648 Carboxylic Acid Oxidase Activity in Shoots of Flooded Tomato Plants Raises Ethylene Production to  
649 Physiologically Active Levels. *Plant Physiology*, 109(4), 1435–1440.  
650 <https://doi.org/10.1104/pp.109.4.1435>
- 651 Evans, D. E. (2004). Aerenchyma formation. *New Phytologist*, 161(1), 35–49.  
652 <https://doi.org/10.1046/j.1469-8137.2003.00907.x>
- 653 Geldhof, B., Pattyn, J., Eyland, D., Carpentier, S., & Van de Poel, B. (2021). A digital sensor to measure real-  
654 time leaf movements and detect abiotic stress in plants. *Plant Physiology*, 187(3), 1131–1148.  
655 <https://doi.org/10.1093/plphys/kiab407>
- 656 Grichko, V. P., & Glick, B. R. (2001). Ethylene and flooding stress in plants. *Plant Physiology and*  
657 *Biochemistry*, 39(1), 1–9. [https://doi.org/10.1016/S0981-9428\(00\)01213-4](https://doi.org/10.1016/S0981-9428(00)01213-4)
- 658 Groeneveld, H. W., & Voeselek, L. A. C. J. (2003). Submergence-induced petiole elongation in *Rumex*  
659 *palustris* is controlled by developmental stage and storage compounds. *Plant and Soil*, 253(1), 115–  
660 123. <https://doi.org/10.1023/A:1024511232626>
- 661 Hackett, R. M., Ho, C., Lin, Z., Foote, H. C. C., Fray, R. G., & Grierson, D. (2000). Antisense Inhibition of the  
662 Nr Gene Restores Normal Ripening to the Tomato Never-ripe Mutant, Consistent with the Ethylene  
663 Receptor- Inhibition Model. *Plant Physiology*, 124(3), 1079–1086.  
664 <https://doi.org/10.1104/pp.124.3.1079>
- 665 Hopper, D. W., Ghan, R., & Cramer, G. R. (2014). A rapid dehydration leaf assay reveals stomatal response

- 666 differences in grapevine genotypes. *Horticulture Research*, 1(October 2013), 1–8.  
667 <https://doi.org/10.1038/hortres.2014.2>
- 668 Horton, R. F. (1992). Submergence-promoted growth of petioles of *Ranunculus pygmaeus* Wahl. *Aquatic*  
669 *Botany*, 44(1), 23–30. [https://doi.org/10.1016/0304-3770\(92\)90078-W](https://doi.org/10.1016/0304-3770(92)90078-W)
- 670 Houben, M., & Van de Poel, B. (2019). 1-aminocyclopropane-1-carboxylic acid oxidase (ACO): The enzyme  
671 that makes the plant hormone ethylene. *Frontiers in Plant Science*, 10(May), 1–15.  
672 <https://doi.org/10.3389/fpls.2019.00695>
- 673 Hsu, F. C., Chou, M. Y., Peng, H. P., Chou, S. J., & Shih, M. C. (2011). Insights into hypoxic systemic responses  
674 based on analyses of transcriptional regulation in arabidopsis. *PLoS ONE*, 6(12), 14–16.  
675 <https://doi.org/10.1371/journal.pone.0028888>
- 676 Hunter, D. a, Yoo, S. D., Butcher, S. M., & McManus, M. T. (1999). Expression of 1-aminocyclopropane-1-  
677 carboxylate oxidase during leaf ontogeny in white clover. *Plant Physiology*, 120(1), 131–142.  
678 <https://doi.org/10.1104/pp.120.1.131>
- 679 Jackson, M. B., & Campbell, D. J. (1976). Waterlogging and Petiole Epinasty in Tomato: the Role of Ethylene  
680 and Low Oxygen. *New Phytologist*, 76(1), 21–29. [https://doi.org/10.1111/j.1469-](https://doi.org/10.1111/j.1469-8137.1976.tb01434.x)  
681 [8137.1976.tb01434.x](https://doi.org/10.1111/j.1469-8137.1976.tb01434.x)
- 682 Jin, S., Hou, B., & Zhang, G. (2021). The ectopic expression of Arabidopsis glucosyltransferase UGT74D1  
683 affects leaf positioning through modulating indole-3-acetic acid homeostasis. *Scientific Reports*,  
684 11(1), 1–13. <https://doi.org/10.1038/s41598-021-81016-x>
- 685 Jordan, W. R., Brown, K. W., & Thomas, J. C. (1975). Leaf Age as a Determinant in Stomatal Control of  
686 Water Loss from Cotton during Water Stress. *Plant Physiology*, 56(5), 595–599.  
687 <https://doi.org/10.1104/pp.56.5.595>
- 688 Kanojia, A., Gupta, S., Benina, M., Fernie, A. R., Mueller-Roeber, B., Gechev, T., & Dijkwel, P. P. (2020).  
689 Developmentally controlled changes during Arabidopsis leaf development indicate causes for loss of  
690 stress tolerance with age. *Journal of Experimental Botany*, 71(20), 6340–6354.  
691 <https://doi.org/10.1093/JXB/ERAA347>
- 692 Kawase, M. (1974). Role of Ethylene in Induction of Flooding Damage in Sunflower. *Physiologia Plantarum*,  
693 31(1), 29–38. <https://doi.org/https://doi.org/10.1111/j.1399-3054.1974.tb03673.x>



- 694 Kazemi, S., & Kefford, N. P. (1974). Apical correlative effects in leaf epinasty of tomato. *Plant Physiology*,  
695 54(4), 512–519. <https://doi.org/10.1104/pp.54.4.512>
- 696 Keller, C. P., & Van Volkenburgh, E. (1997). Auxin-Induced Epinasty of Tobacco Leaf Tissues (A  
697 Nonethylene-Mediated Response). *Plant Physiology*, 113(1 997), 603–610.  
698 <https://doi.org/10.1104/pp.113.2.603>
- 699 Kende, H., Van Knaap, E. Der, & Cho, H. T. (1998). Deepwater rice: A model plant to study stem elongation.  
700 *Plant Physiology*, 118(4), 1105–1110. <https://doi.org/10.1104/pp.118.4.1105>
- 701 Kim, J. H., Woo, H. R., Kim, J., Lim, P. O., Lee, I. C., Choi, S. H., Hwang, D., & Nam, H. G. (2009). Trifurcate  
702 Feed-Forward Regulation of Age-Dependent Cell Death Involving miR164 in Arabidopsis. *Science*,  
703 323(5917), 1053–1057. <https://doi.org/10.1126/science.1166386>
- 704 Kuhn, B. M., Geisler, M., Bigler, L., & Ringli, C. (2011). Flavonols accumulate asymmetrically and affect  
705 auxin transport in arabidopsis. *Plant Physiology*, 156(2), 585–595.  
706 <https://doi.org/10.1104/pp.111.175976>
- 707 Kuhn, B. M., Nodzyński, T., Errafi, S., Bucher, R., Gupta, S., Aryal, B., Dobrev, P., Bigler, L., Geisler, M.,  
708 Zažímalová, E., Friml, J., & Ringli, C. (2017). Flavonol-induced changes in PIN2 polarity and auxin  
709 transport in the Arabidopsis thaliana rol1-2 mutant require phosphatase activity. *Scientific Reports*,  
710 7(January), 1–13. <https://doi.org/10.1038/srep41906>
- 711 Lanahan, M. B., Yen Hsiao Ching, Giovannoni, J. J., & Klee, H. J. (1994). The Never ripe mutation blocks  
712 ethylene perception in tomato. *Plant Cell*, 6(4), 521–530. <https://doi.org/10.1105/tpc.6.4.521>
- 713 Lee, Y., Jung, J. W., Kim, S. H. S. K. S. H., Hwang, Y. S., Lee, J. S., & Kim, S. H. S. K. S. H. (2008). Ethylene-  
714 induced opposite redistributions of calcium and auxin are essential components in the development  
715 of tomato petiolar epinastic curvature. *Plant Physiology and Biochemistry*, 46(7), 685–693.  
716 <https://doi.org/10.1016/j.plaphy.2008.04.003>
- 717 Li, Z., Peng, J., Wen, X., & Guo, H. (2013). ETHYLENE-INSENSITIVE3 is a senescence-associated gene that  
718 accelerates age-dependent leaf senescence by directly repressing miR164 transcription in  
719 Arabidopsis. *Plant Cell*, 25(9), 3311–3328. <https://doi.org/10.1105/tpc.113.113340>
- 720 Lin, Z., Arciga-Reyes, L., Zhong, S., Alexander, L., Hackett, R., Wilson, I., & Grierson, D. (2008). SITPR1, a  
721 tomato tetratricopeptide repeat protein, interacts with the ethylene receptors NR and LeETR1,

- 722 modulating ethylene and auxin responses and development. *Journal of Experimental Botany*, 59(15),  
723 4271–4287. <https://doi.org/10.1093/jxb/ern276>
- 724 Liu, M., Chen, Y., Chen, Y., Shin, J. H., Mila, I., Audran, C., Zouine, M., Pirrello, J., & Bouzayen, M. (2018).  
725 The tomato Ethylene Response Factor Sl-ERF.B3 integrates ethylene and auxin signaling via direct  
726 regulation of Sl-Aux/IAA27. *New Phytologist*, 219(2), 631–640. <https://doi.org/10.1111/nph.15165>
- 727 Lizada, M. C., & Yang, S. F. (1979). A simple and sensitive assay for 1-aminocyclopropane-1-carboxylic acid.  
728 *Analytical Biochemistry*, 100(1), 140–145. [https://doi.org/10.1016/0003-2697\(79\)90123-4](https://doi.org/10.1016/0003-2697(79)90123-4)
- 729 Ljung, K., Bhalerao, R. P., & Sandberg, G. (2002). Sites and homeostatic control of auxin biosynthesis in  
730 Arabidopsis during vegetative growth. *The Plant Journal*, 28(4), 465–474.  
731 <https://doi.org/10.1046/j.1365-313X.2001.01173.x>
- 732 Lyon, C. J. (1963a). Auxin Factor in Branch Epinasty. *Plant Physiology*, 38(2), 145–152.  
733 <https://doi.org/10.1104/pp.38.2.145>
- 734 Lyon, C. J. (1963b). Auxin Transport in Leaf Epinasty. *Plant Physiology*, 38(5), 567–574.  
735 <https://doi.org/10.1104/pp.38.5.567>
- 736 Maloney, G. S., DiNapoli, K. T., & Muday, G. K. (2014a). The anthocyanin reduced Tomato Mutant  
737 Demonstrates the Role of Flavonols in Tomato Lateral Root and Root Hair Development. *Plant*  
738 *Physiology*, 166(2), 614–631. <https://doi.org/10.1104/pp.114.240507>
- 739 Maloney, G. S., DiNapoli, K. T., & Muday, G. K. (2014b). The anthocyanin reduced Tomato Mutant  
740 Demonstrates the Role of Flavonols in Tomato Lateral Root and Root Hair Development. *Plant*  
741 *Physiology*, 166(2), 614–631. <https://doi.org/10.1104/pp.114.240507>
- 742 Marias, D. E., Meinzer, F. C., & Still, C. (2017). Impacts of leaf age and heat stress duration on  
743 photosynthetic gas exchange and foliar nonstructural carbohydrates in *Coffea arabica*. *Ecology and*  
744 *Evolution*, 7(4), 1297–1310. <https://doi.org/10.1002/ece3.2681>
- 745 Muday, G. K., Rahman, A., & Binder, B. M. (2012). Auxin and ethylene: collaborators or competitors?  
746 *Trends in Plant Science*, 17(4), 181–195. <https://doi.org/10.1016/j.tplants.2012.02.001>
- 747 Murray, T. A., & Mcmanus, M. T. (2005). Developmental regulation of 1-aminocyclopropane-1-carboxylate  
748 synthase gene expression during leaf ontogeny in white clover. *Physiologia Plantarum*, 124(1), 107–  
749 120. <https://doi.org/10.1111/j.1399-3054.2005.00494.x>

- 750 Negi, S., Sukumar, P., Liu, X., Cohen, J. D., & Muday, G. K. (2010). Genetic dissection of the role of ethylene  
751 in regulating auxin-dependent lateral and adventitious root formation in tomato. *Plant Journal*,  
752 *61*(1), 3–15. <https://doi.org/10.1111/j.1365-313X.2009.04027.x>
- 753 Nghi, K. N., Tagliani, A., Mariotti, L., Weits, D. A., Perata, P., & Pucciariello, C. (2021). Auxin is required for  
754 the long coleoptile trait in japonica rice under submergence. *New Phytologist*, *229*(1), 85–93.  
755 <https://doi.org/10.1111/nph.16781>
- 756 Noh, B., Murphy, A. S., & Spalding, E. P. (2001). Multidrug resistance-like genes of Arabidopsis required  
757 for auxin transport and auxin-mediated development. *Plant Cell*, *13*(11), 2441–2454.  
758 <https://doi.org/10.1105/tpc.13.11.2441>
- 759 Olson, D. C., Oetiker, J. H., & Yang, S. F. (1995). Analysis of LE-ACS3, a 1-Aminocyclopropane-1-carboxylic  
760 Acid Synthase Gene Expressed during Flooding in the Roots of Tomato Plants. *Journal of Biological*  
761 *Chemistry*, *270*(23), 14056–14061. <https://doi.org/10.1074/jbc.270.23.14056>
- 762 Park, Y. J., Lee, H. J., Gil, K. E., Kim, J. Y., Lee, J. H., Lee, H., Cho, H. T., Vu, L. D., Smet, I. De, & Park, C. M.  
763 (2019). Developmental programming of therrnonastic leaf movement. *Plant Physiology*, *180*(2),  
764 1185–1197. <https://doi.org/10.1104/pp.19.00139>
- 765 Pattison, R. J., & Catalá, C. (2012). Evaluating auxin distribution in tomato (*Solanum lycopersicum*) through  
766 an analysis of the PIN and AUX/LAX gene families. *Plant Journal*, *70*(4), 585–598.  
767 <https://doi.org/10.1111/j.1365-313X.2011.04895.x>
- 768 Pattyn, J., Vaughan-Hirsch, J., & Van de Poel, B. (2021). The regulation of ethylene biosynthesis: a complex  
769 multilevel control circuitry. *New Phytologist*, *229*(2), 770–782. <https://doi.org/10.1111/nph.16873>
- 770 Pazmiño, D. M., Rodríguez-Serrano, M., Romero-Puertas, M. C., Archilla-Ruiz, A., Del Río, L. A., & Sandalio,  
771 L. M. (2011). Differential response of young and adult leaves to herbicide 2,4-dichlorophenoxyacetic  
772 acid in pea plants: role of reactive oxygen species. *Plant, Cell & Environment*, *34*(11), 1874–1889.  
773 <https://doi.org/10.1111/j.1365-3040.2011.02383.x>
- 774 Pazmiño, D. M., Rodríguez-Serrano, M., Sanz, M., Romero-Puertas, M. C., & Sandalio, L. M. (2014).  
775 Regulation of epinasty induced by 2,4-dichlorophenoxyacetic acid in pea and Arabidopsis plants.  
776 *Plant Biology*, *16*(4), 809–818. <https://doi.org/10.1111/plb.12128>
- 777 Pierik, R., Tholen, D., Poorter, H., Visser, E. J. W., & Voeselek, L. A. C. J. (2006). The Janus face of ethylene:

- 778 growth inhibition and stimulation. *Trends in Plant Science*, 11(4), 176–183.  
779 <https://doi.org/10.1016/j.tplants.2006.02.006>
- 780 Rankenberg, T., Geldhof, B., van Veen, H., Holsteens, K., Van de Poel, B., & Sasidharan, R. (2021). Age-  
781 Dependent Abiotic Stress Resilience in Plants. *Trends in Plant Science*, 26(7), 692–705.  
782 <https://doi.org/10.1016/j.tplants.2020.12.016>
- 783 Rauf, M., Arif, M., Fisahn, J., Xue, G.-P., Balazadeh, S., & Mueller-Roeber, B. (2013). NAC Transcription  
784 Factor SPEEDY HYPONASTIC GROWTH Regulates Flooding-Induced Leaf Movement in Arabidopsis.  
785 *The Plant Cell*, 25(12), 4941–4955. <https://doi.org/10.1105/tpc.113.117861>
- 786 Romano, C. P., Cooper, M. L., & Klee, H. J. (1993). Uncoupling Auxin and Ethylene Effects in Transgenic  
787 Tobacco and Arabidopsis Plants. *The Plant Cell*, 5(2), 181–189. <https://doi.org/10.1105/tpc.5.2.181>
- 788 Sandalio, L. M., Rodríguez-Serrano, M., & Romero-Puertas, M. C. (2016). Leaf epinasty and auxin: A  
789 biochemical and molecular overview. *Plant Science*, 253(October), 187–193.  
790 <https://doi.org/10.1016/j.plantsci.2016.10.002>
- 791 Sasidharan, R., Bailey-Serres, J., Ashikari, M., Atwell, B. J., Colmer, T. D., Fagerstedt, K., Fukao, T.,  
792 Geigenberger, P., Hebelstrup, K. H., Hill, R. D., Holdsworth, M. J., Ismail, A. M., Licausi, F., Mustroph,  
793 A., Nakazono, M., Pedersen, O., Perata, P., Sauter, M., Shih, M. C., ... Voesenek, L. A. C. J. (2017).  
794 Community recommendations on terminology and procedures used in flooding and low oxygen  
795 stress research. In *New Phytologist*. <https://doi.org/10.1111/nph.14519>
- 796 Shimamura, S., Yamamoto, R., Nakamura, T., Shimada, S., & Komatsu, S. (2010). Stem hypertrophic  
797 lenticels and secondary aerenchyma enable oxygen transport to roots of soybean in flooded soil.  
798 *Annals of Botany*, 106(2), 277–284. <https://doi.org/10.1093/aob/mcq123>
- 799 Shiu, O. Y., Oetiker, J. H., Yip, W. K., & Yang, S. F. A. (1998). The promoter of LE-ACS7, an early flooding-  
800 induced 1-aminocyclopropane-1-carboxylate synthase gene of the tomato, is tagged by a Sol3  
801 transposon. *Proceedings of the National Academy of Sciences of the United States of America*, 95(17),  
802 10334–10339. <https://doi.org/10.1073/pnas.95.17.10334>
- 803 Šimura, J., Antoniadi, I., Široká, J., Tarkowská, D., Strnad, M., Ljung, K., & Novák, O. (2018). Plant  
804 hormonomics: Multiple phytohormone profiling by targeted metabolomics. *Plant Physiology*,  
805 177(2), 476–489. <https://doi.org/10.1104/pp.18.00293>

- 806 Stewart, E. R., & Freebairn, H. T. (1969). Ethylene, seed germination, and epinasty. *Plant Physiology*, *44*(7),  
807 955–958. <https://doi.org/10.1104/pp.44.7.955>
- 808 Tonneijck, A. E. G., Berge, W. F. te., Jansen, B. P., & Bakker, C. (1999). Epinastic response of potato to  
809 atmospheric ethylene near polyethylene manufacturing plants. *Chemosphere*, *39*(10), 1617–1628.  
810 [https://doi.org/10.1016/S0045-6535\(99\)00060-0](https://doi.org/10.1016/S0045-6535(99)00060-0)
- 811 Ursin, V. M., & Bradford, K. J. (1989a). Auxin and Ethylene Regulation of Petiole Epinasty in Two  
812 Developmental Mutants of Tomato, diageotropica and Epinastic. *Plant Physiology*, *90*, 1341–1346.  
813 <https://doi.org/10.1104/pp.90.4.1341>
- 814 Ursin, V. M., & Bradford, K. J. (1989b). Auxin and Ethylene Regulation of Petiole Epinasty in Two  
815 Developmental Mutants of Tomato, diageotropica and Epinastic. *Plant Physiology*, *90*(SEPTEMBER),  
816 1341–1346. <https://doi.org/10.1104/pp.90.4.1341>
- 817 van de Poel, B., Bulens, I., Markoula, A., Hertog, M. L. A. T. M., Dreesen, R., Wirtz, M., Vandoninck, S.,  
818 Oppermaun, Y., Keulemans, J., Hell, R., Waelkens, E., de Proft, M. P., Sauter, M., Nicolai, B. M., &  
819 Geeraerd, A. H. (2012). Targeted systems biology profiling of tomato fruit reveals coordination of  
820 the Yang cycle and a distinct regulation of ethylene biosynthesis during postclimacteric ripening.  
821 *Plant Physiology*, *160*(3), 1498–1514. <https://doi.org/10.1104/pp.112.206086>
- 822 Van de Poel, B., Smet, D., & Van Der Straeten, D. (2015). Ethylene and hormonal cross talk in vegetative  
823 growth and development. *Plant Physiology*, *169*(1), 61–72. <https://doi.org/10.1104/pp.15.00724>
- 824 Van de Poel, B., Vandenzavel, N., Smet, C., Nicolay, T., Bulens, I., Mellidou, I., Vandoninck, S., Hertog, M.  
825 L. A. T. M., Derua, R., Spaepen, S., Vanderleyden, J., Waelkens, E., De Proft, M. P., Nicolai, B. M., &  
826 Geeraerd, A. H. (2014). Tissue specific analysis reveals a differential organization and regulation of  
827 both ethylene biosynthesis and E8 during climacteric ripening of tomato. *BMC Plant Biology*, *14*(1).  
828 <https://doi.org/10.1186/1471-2229-14-11>
- 829 Van Geest, G., Van Ieperen, W., Post, A. G., & Schoutsen, C. G. L. M. (2012). Leaf epinasty in  
830 chrysanthemum: Enabling breeding against an adverse trait by physiological research. *Acta*  
831 *Horticulturae*, *953*, 345–350.
- 832 Vandebussche, F., Vriezen, W. H., Smalle, J., Laarhoven, L. J. J., Harren, F. J. M., & Van Der Straeten, D.  
833 (2003). Ethylene and Auxin Control the Arabidopsis Response to Decreased Light Intensity. *Plant*  
834 *Physiology*, *133*(2), 517–527. <https://doi.org/10.1104/pp.103.022665>

- 835 Ventura, I., Brunello, L., Iacopino, S., Valeri, M. C., Novi, G., Dornbusch, T., Perata, P., & Loreti, E. (2020).  
836 Arabidopsis phenotyping reveals the importance of alcohol dehydrogenase and pyruvate  
837 decarboxylase for aerobic plant growth. *Scientific Reports*, *10*(1), 1–14.  
838 <https://doi.org/10.1038/s41598-020-73704-x>
- 839 Vidoz, M. L., Mignolli, F., Aispuru, H. T., & Mroginski, L. A. (2016). Rapid formation of adventitious roots  
840 and partial ethylene sensitivity result in faster adaptation to flooding in the aerial roots (aer) mutant  
841 of tomato. *Scientia Horticulturae*, *201*, 130–139. <https://doi.org/10.1016/j.scienta.2016.01.032>
- 842 Voeselek, L. A. C. J., Rijnders, J. H. G. M., Peeters, A. J. M., van de Steeg, H. M., & de Kroon, H. (2004).  
843 PLANT HORMONES REGULATE FAST SHOOT ELONGATION UNDER WATER: FROM GENES TO  
844 COMMUNITIES. *Ecology*, *85*(1), 16–27. <https://doi.org/10.1890/02-740>
- 845 Wiese, M. V, & Devay, J. E. (1970). Growth Regulator Changes in Cotton Associated with Defoliation  
846 Caused by Verticillium albo-atrum. *Plant Physiology*, *45*(3), 304–309.  
847 <https://doi.org/10.1104/pp.45.3.304>
- 848 Xu, Q., Krishnan, S., Merewitz, E., Xu, J., & Huang, B. (2016). Gibberellin-Regulation and Genetic Variations  
849 in Leaf Elongation for Tall Fescue in Association with Differential Gene Expression Controlling Cell  
850 Expansion. *Scientific Reports*, *6*(June), 1–12. <https://doi.org/10.1038/srep30258>
- 851 Young, T. E., Meeley, R. B., & Gallie, D. R. (2004). ACC synthase expression regulates leaf performance and  
852 drought tolerance in maize. *Plant Journal*, *40*(5), 813–825. [https://doi.org/10.1111/j.1365-](https://doi.org/10.1111/j.1365-313X.2004.02255.x)  
853 [313X.2004.02255.x](https://doi.org/10.1111/j.1365-313X.2004.02255.x)
- 854